



Article

Molecular and Histologic Adaptation of Horned Gall Induced by the Aphid *Schlechtendalia chinensis* (Pemphigidae)

Qin Lu ¹ , Xiaoming Chen ^{1,2}, Zixiang Yang ¹ , Nawaz Haider Bashir ¹, Juan Liu ¹, Yongzhong Cui ¹, Shuxiao Shao ¹, Ming-Shun Chen ³ and Hang Chen ^{1,2,*}

¹ Research Institute of Resource Insects, Chinese Academy of Forestry, Kunming 650224, China; luqin_19900319@163.com (Q.L.); cafcxm@139.com (X.C.); yzx1019@163.com (Z.Y.); haiderynau170@yahoo.com (N.H.B.); liujuan301@126.com (J.L.); cafkmcyz@126.com (Y.C.); shuxiashao@126.com (S.S.)

² The Key Laboratory of Cultivating and Utilization of Resources Insects of State Forestry Administration, Kunming 650224, China

³ Department of Entomology, Kansas State University, 123 Waters Hall, Manhattan, KS 66506, USA; mchen@ksu.edu

* Correspondence: stuchen6481@gmail.com

Abstract: Chinese galls are the result of hyperplasia in host plants induced by aphids. The metabolism and gene expression of these galls are modified to accommodate the aphids. Here, we highlight the molecular and histologic features of horned galls according to transcriptome and anatomical structures. In primary pathways, genes were found to be unevenly shifted and selectively expressed in the galls and leaves near the galls (LNG). Pathways for amino acid synthesis and degradation were also unevenly shifted, favoring enhanced accumulation of essential amino acids in galls for aphids. Although galls enhanced the biosynthesis of glucose, which is directly available to aphids, glucose content in the gall tissues was lower due to the feeding of aphids. Pathways of gall growth were up-regulated to provide enough space for aphids. In addition, the horned gall has specialized branched schizogenous ducts and expanded xylem in the stalk, which provide a broader feeding surface for aphids and improve the efficiency of transportation and nutrient exchange. Notably, the gene expression in the LNG showed a similar pattern to that of the galls, but on a smaller scale. We suppose the aphids manipulate galls to their advantage, and galls lessen competition by functioning as a medium between the aphids and their host plants.

Keywords: plant-insect interaction; horned gall; transcriptome; nutrition supply; co-evolution



Citation: Lu, Q.; Chen, X.; Yang, Z.; Bashir, N.H.; Liu, J.; Cui, Y.; Shao, S.; Chen, M.-S.; Chen, H. Molecular and Histologic Adaptation of Horned Gall Induced by the Aphid *Schlechtendalia chinensis* (Pemphigidae). *Int. J. Mol. Sci.* **2021**, *22*, 5166. <https://doi.org/10.3390/ijms22105166>

Academic Editor: Maurizio Chiurazzi

Received: 22 March 2021

Accepted: 11 May 2021

Published: 13 May 2021

Publisher's Note: MDPI stays neutral with regard to jurisdictional claims in published maps and institutional affiliations.



Copyright: © 2021 by the authors. Licensee MDPI, Basel, Switzerland. This article is an open access article distributed under the terms and conditions of the Creative Commons Attribution (CC BY) license (<https://creativecommons.org/licenses/by/4.0/>).

1. Introduction

Plant galls are outgrowths of various plant tissues after stimulation by organisms ranging from insects to bacteria. They are outcomes of the interaction between parasites and their host plants [1]. In contrast to normal tissues, parasites are able to control the gall to suit the parasite's needs. Thus, plant galls have long been considered an extension of the inducer's phenotype [2]. In some species of galling bacteria, the galls' development is based on DNA transference; however, the exact mechanism remains obscure in the case of galls induced by insects [3,4].

The galls have many specialized structures and functions to enhance parasite fitness, according to three main hypotheses. First, completely closed galls can resist the invasion of pathogenic microorganisms and the predation of natural enemies (i.e., defense hypothesis) [5–7]. Second, the gall is a sink of photosynthate that can accumulate and store nutrients, and then provide the necessary nutrients for the growth and development of galling insects by intercepting organic matter and the accumulation of inorganic nutrients (i.e., nutrition hypothesis) [8]. Third, the gall is a microenvironment that protects the inducers against inclement weather (i.e., microenvironment hypothesis) [9,10].

The gall offers many advantages to the inducer, and some galls also benefit the host plant. The gall can be a deterrent that protects plant leaves from chewing by herbivores because of abundant tannins, such as galls induced by *Rectinasus buxtoni* on *Pistacia palaestina* [11]. A similar phenomenon occurs in galls present in the leaflets induced by genus *Pistacia* [12]. Thus, in some cases, the gall may be considered a reward from the inducer [13]. These studies indicate that galling insects should not be simply regraded as harmful parasites, and that more complex symbiotic relationships exist between some inducers and their host plants.

“The insect galls are in a sense new plant organs because it is the plant that produces the gall in response to a specific stimulus provided by the invading insect” [14]. The metabolism of galls is different from that of normal organs and can affect the host plants [15]. The impact of galls on host plants varies widely by species under different conditions. Some gall inducers are able to stimulate the photosynthetic rates of nearby tissues by increasing sink demand [16,17]. By comparison, a few gall inducers are known to reduce photosynthetic rates of nearby tissues of host plants [18,19]. In addition to the impact on host photosynthesis, gall inducers can alter various metabolic pathways in host plants in different ways [20]. Gall inducers can also suppress or promote host defense reactions, depending on the types of gall inducer and host plant [21].

Horned galls on *Rhus chinensis* induced by the aphid *Schlechtendalia chinensis* possess a number of interesting traits, namely, they are larger, are clustered on small leaf wings, and are an important economic product containing a large quantity of tannins [22,23]. Notably, a horned gall can host thousands of aphids at the later stage of development [24], and a high concentration of CO₂ is accumulated within the gall because of the respiration of these aphids. This CO₂ is useful for host plants and is transported to nearby leaves to enhance their photosynthetic efficiency. Thus, the negative effect of aphid feeding is ultimately reduced. In addition, the inner surface of the horned gall is able to absorb and reuse honeydew. Due to the combination of photosynthesis and honeydew recycling, the *S. chinensis*–*R. chinensis* system is highly efficient. During the long period of coevolution between *S. chinensis* and *R. chinensis*, the horned gall has developed a complex nutrient exchange mechanism with its host plant via sophisticated metabolism [25].

In this study, we aimed to examine the molecular and histologic basis in galls for the mutualism developed between *S. chinensis* and *R. chinensis* through adaptive coevolution. Specifically, we examined changes in various metabolic pathways in galls by comparing tissues from LNG with tissues from leaves without nearby galls (LWG) via transcriptomic analyses.

2. Results

2.1. Morphological and Histologic Structures of Horned Galls

Horned galls were located on rachis wings of the plant *R. chinensis* and induced by the aphid *S. chinensis* (Figure 1a,b). They were initially small and round, but multiple galls with irregular shapes reached a large size and could completely cover a rachis wing at a later stage (Figure 1a,b). A horned gall was connected to a rachis wing via a highly lignified base region (stalk) (Figure 1b), which had expanded xylem and ducts (Figure 1d). Aphids lived in a closed gall and fed on the inner wall of the gall (Figure 1c). Compared with galls induced by other aphids, horned galls were significantly larger and more clustered on rachis wings. A small rachis wing could carry up to 19 (12 ± 6.34) galls. To accommodate such a large number of feeding aphids, branch schizogenous ducts were present on the inner surface (Figure 1f,g) and were surrounded by densely arranged parenchyma cells and associated with vascular cells (Figure 1e). The schizogenous ducts were branched and filled the inner wall (Figure 1f,g). This was clearly different from the normal leaf structure. Tissues of the leaf showed obvious differentiation among cells, such as upper and lower epithelial cells, palisade cells, and spongy cells. The palisade and spongy cells were closely arranged in the initial stage, and they became loose and porous in the mature stage (Figure 1k,l). The inner wall was rough and characterized by a large number of holes

(Figure 1h), and abundant tomentum and stoma were found on the surface of the outer wall (Figure 1i). The stylophores left by feeding aphids were present on the schizogenous ducts and vascular bundles (Figure 1j).

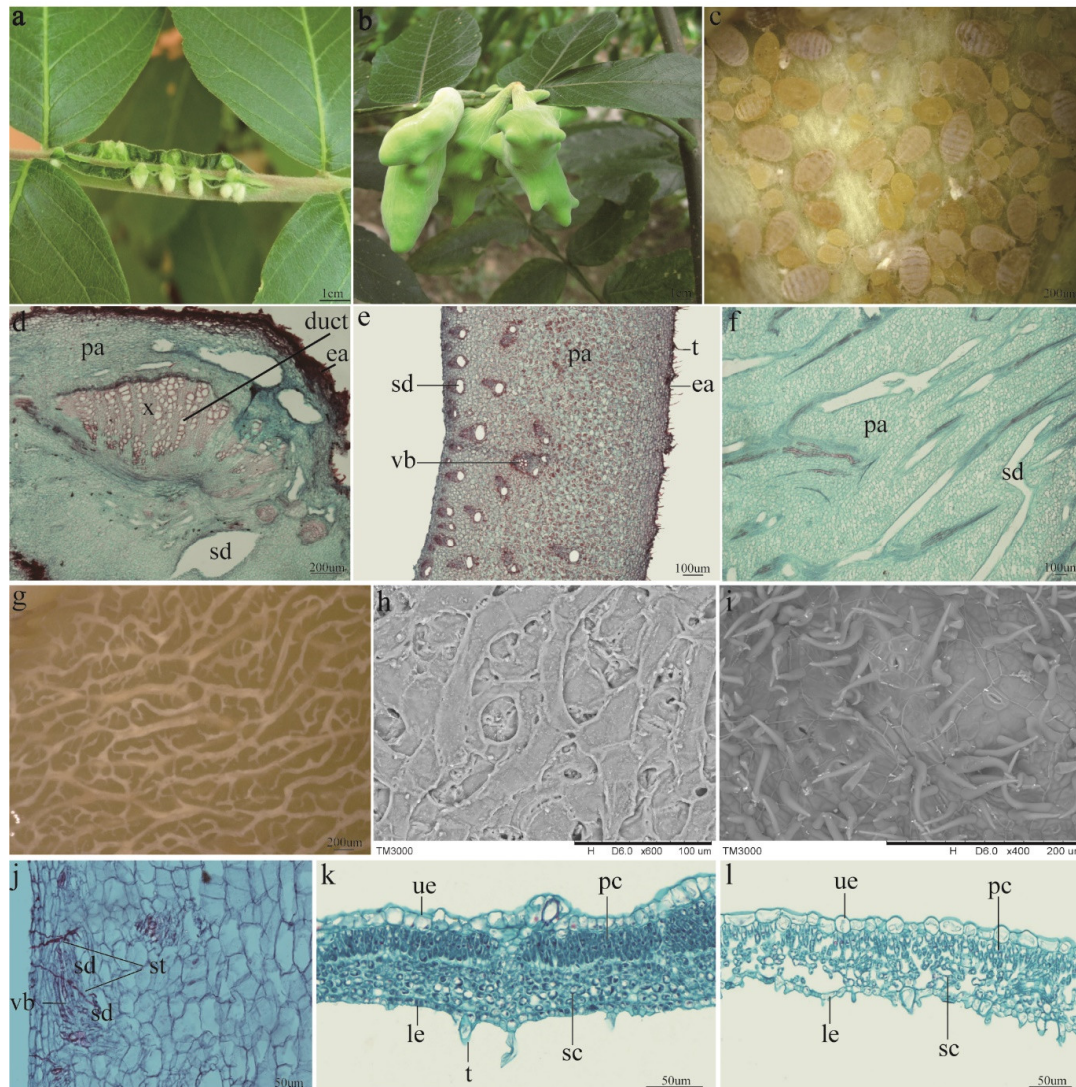


Figure 1. Localization, morphology, and anatomical structure of the horned gall. (a) Young horned galls clustered on rachis wings. (b) Mature galls connected with rachis leaf wing via a specialized stalk. (c) Aphids feeding on inner wall. (d) Cross-section of the stalk. Many ducts are present in the expanded xylem. (e) Crosscutting of the gall wall. The wall comprises parenchyma cells and contains many vascular bundles that are joined to the schizogenous ducts. (f) Plane surface of the horned gall; long schizogenous ducts are present. (g) The inner surface of the horned gall treated by NaOH. Vast, branched schizogenous ducts are present in the inner wall. (h) A scanning electron microscope (SEM) image of the inner surface. The inner wall was rough and characterized by holes. (i) The outer surface of the horned gall in the SEM image. Stoma and tomentum are present in the outer wall. (j) The stylophores of the aphids. Stylophores gathered in the vascular bundle of the horned gall. (k) The cross-section of the young *R. chinensis* leaf. The palisade and spongy cells are closely arranged. (l) The cross-section of the mature *R. chinensis* leaf. The cells, particularly the spongy tissues, are loose and porous. ea = epidermis-air, x = xylem, pa = parenchyma, sd = schizogenous duct, vb = vascular bundle, t = tomentum, st = stylophore, el = epidermis-lumen, pc = palisade cell, sc = spongy cell, le = lower epithelial cell, ue = upper epithelial cell.

2.2. Changes in the Abundance of Selected Cofactors and Nutrients

Nicotinamide adenine dinucleotide (NAD⁺) is a cofactor that is central to metabolism. The abundance of NAD⁺, and its reduced form NADH, in addition to nicotinamide adenine

dinucleotide phosphates NADP⁺ and NADPH, was determined in galls, LNG, and LWG (Table 1). The abundance of NAD⁺ and NADH was at least three-fold higher in gall tissues than in the two kinds of leaf tissues. The abundance of NADP⁺ was not significantly different among the different samples. However, the abundance of NADPH was more than two-fold higher in galls compared with samples from leaves with or without galls. No significant difference in the abundance of the cofactors was observed between samples from LNG and LWG, except NAD⁺, which was lower in LWG than in LNG.

Table 1. The content of coenzymes in the different samples.

Coenzymes	Gall	LWG	LNG
NAD ⁺ (nmol\g)	142.74 ± 9.17 ^a	30.57 ± 1.28 ^c	42.62 ± 6.68 ^b
NADH (nmol\g)	108.75 ± 9.94 ^a	27.07 ± 2.29 ^b	30.35 ± 6.44 ^b
NADP ⁺ (nmol\g)	12.46 ± 2.01 ^a	12.13 ± 0.49 ^a	11.72 ± 0.37 ^a
NADPH (nmol\g)	36.77 ± 11.21 ^a	15.15 ± 1.48 ^b	15.86 ± 0.92 ^b

Note: different letters in the same row represent the significant difference at the level of $p < 0.05$.

Total proteins, fat, and starch—the three major types of energy reserves and nutrients—were also determined in galls and compared with those in leaf tissues (Table 2). Total proteins and fat were at least three-fold less in galls than in leaf-tissue samples. However, starch was significantly higher in galls than in leaf tissues. In contrast, the abundance of simple sugars including fructose, glucose, and sucrose was significantly less in galls than in leaf tissues (Table 2). No significant or marginal differences in nutrients were observed between LNG and LWG.

Table 2. The percentage of different types of nutrients in dried tissues.

Nutrients	Gall	LWG	LNG
Protein (%)	3.28 ± 0.18 ^b	11.18 ± 0.03 ^a	11.19 ± 0.09 ^a
Fat (%)	1.64 ± 0.13 ^b	3.61 ± 0.18 ^a	3.83 ± 0.37 ^a
Starch (%)	2.51 ± 0.06 ^a	1.83 ± 0.07 ^b	1.02 ± 0.05 ^c
Fructose (%)	0.91 ± 0.04 ^c	3.31 ± 0.03 ^a	2.52 ± 0.04 ^b
Glucose (%)	0.94 ± 0.001 ^c	2.17 ± 0.03 ^a	1.82 ± 0.001 ^b
Sucrose (%)	1.29 ± 0.02 ^b	2.50 ± 0.12 ^a	2.40 ± 0.02 ^a

Note: different letters in the same row represent the significant difference at the level of $p < 0.05$.

2.3. Changes in Gene Expression of Major Metabolic Pathways in Galls

To analyze the changes in gene expression of major metabolic pathways, RNA sequencing (RNA-seq) was conducted with samples from galls, LNG, and LWG. A total of 112,543 unigenes covering a total of 127,567,799 nucleotides were obtained from the combined samples. The average length of the high-quality reads was 1133 bp. High-quality reads were assembled into unigenes that covered 45 megabases with 1032 nucleotide residues (nt) in average size and N50 1746 nt. Statistics of sequence reads and assembled unigenes are shown in Tables A1–A4. Unigenes were annotated against non-redundant protein sequences (Nr), NCBI nucleotide sequences (Nt), the manually annotated and curated protein sequence database (Swiss-Prot), Kyoto Encyclopedia of Genes and Genomes Ortholog database (KEGG), and Clusters of Orthologous Groups of proteins (COG) and Gene Ontology (GO) databases. The annotation results are shown in Table A5.

In terms of the number of differentially expressed genes (DEGs), LNG and LWG showed similar gene expressions, which were different from that of the gall (Figure 2a). Comparative analyses identified 11,891 unigenes were up-regulated and 12,710 unigenes were down-regulated in galls compared with LWG; 10,015 unigenes were up-regulated and 9822 unigenes were down-regulated in galls compared with LNG. In contrast, only 556 unigenes were up-regulated and 781 unigenes were down-regulated in LNG compared with LWG (Figure 2b).

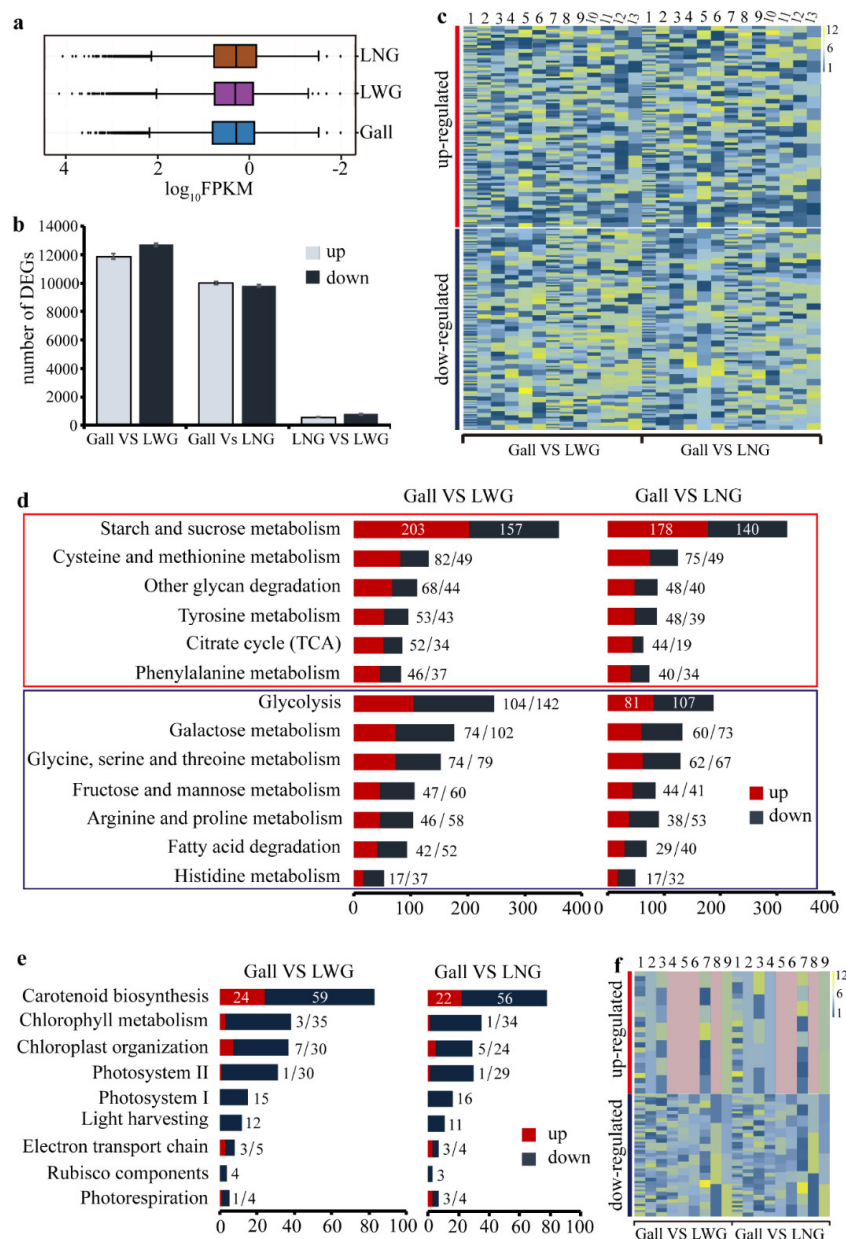


Figure 2. The transcriptomic analysis of the samples. **(a)** Box plot of all gene expressions. **(b)** The number of DEGs in gall vs. LWG, gall vs. LNG, and LNG vs. LWG. **(c)** Heat map of DEGs that regulate metabolism of nutrients in gall vs. LWG (\log_2 FoldChange(Gall/LWG)) and gall vs. LNG (\log_2 FoldChange(Gall/LNG)). Colors from dark blue to yellow reflect smaller to larger differences. A single block represents a single gene in the map. The numbers at the top of the graph represent different functional categories, with 1 representing starch and sucrose metabolism; 2, cysteine and methionine metabolism; 3, other glycan degradation; 4, tyrosine metabolism; 5, citrate cycle (TCA cycle); 6, phenylalanine metabolism; 7, glycolysis; 8, galactose metabolism; 9, glycine, serine and threonine metabolism; 10, fructose and mannose metabolism; 11, arginine and proline metabolism; 12, fatty acid degradation; 13, histidine metabolism. The numerical order corresponds to the ordinate from top to bottom in figure d. **(d)** DEGs involved in nutrient metabolism. The DEGs were identified in pairs of gall vs. LWG and gall vs. LNG. Up-regulated pathways are marked by red rectangles and down-regulated pathways are marked by dark blue rectangles. **(e)** DEGs involved in photosynthesis based on gall vs. LWG and gall vs. LNG comparisons. All subpathways for photosynthesis were down-regulated in gall tissues. **(f)** Heat map of DEGs related to photosynthesis based on LNG vs. LWG (\log_2 FoldChange(LNG/LWG)) comparison. The numbers at the top of the graph represent different subcategories, with 1, carotenoid biosynthesis; 2, chlorophyll metabolism; 3, chloroplast organization; 4, photosystem II; 5, photosystem I; 6, light harvesting; 7, electron transport chain; 8, rubisco components; and 9, photorespiration. Pink represents that no gene was found in this subpathway.

Major metabolic pathways with major changes in gene expression in galls are listed in Table 3. A pathway in which two-thirds of DEGs were up- or down-regulated was considered to be significant. Seven metabolic pathways were significantly down-regulated in gall tissues compared with LWG. The down-regulated pathways included 'photosynthesis', 'pentose-phosphate shunt', 'vitamin biosynthesis', 'iron-sulfur cluster and related metabolism', 'ATP-dependent proteases', and 'disease resistance proteins'. Metabolic pathways that were significantly up-regulated were also present in galls. The up-regulated pathways included 'nucleoside biosynthesis', 'lipid and fatty acid transport', 'vesicle-mediated transport', 'water transport', 'DNA replication and repair', 'histones', 'chromosome structure and maintenance', 'cell cycle', 'cell growth', 'gene silencing', 'tissue development', 'structure', 'ribosomal proteins', 'translation initiation', 'translation elongation', 'response to misfolded proteins', 'response to metal ions', and 'response to salts'. The top ten genes with large differences in all pathways are listed in Table A6.

Table 3. The up- and down-regulated pathways in gall vs. LWG (based on KEGG pathway).

Pathways	Functional Category/Subcategory	Total	Down-Regulated	Up-Regulated	Down/Up
Photosynthesis	Photosynthesis	233	194	39	4.97
Pentose phosphate pathway	Pentose-phosphate shunt	114	78	14	5.57
	Vitamin	29	14	4	3.50
	Iron and sulfate metabolism	47	27	3	9.00
	small molecule metabolism	100	49	18	2.72
	Disease resistance proteins	56	18	9	2.00
	ATP-dependent proteases	27	15	2	7.50
	Cysteine proteases	13	6	3	2.00
Metabolism	Nucleoside metabolism	159	22	59	0.37
	Structure	236	27	129	0.21
Protein synthesis	Ribosomal proteins	193	29	128	0.23
	Translation	275	56	140	0.40
	Initiation	85	16	44	0.37
	Elongation	33	2	17	0.12
	Others	123	22	70	0.31
	Protein myristoylation	39	6	15	0.40
Transport	Lipid and fatty acid transport	60	10	20	0.50
	vesicle-mediated and intracellular transport	105	13	50	0.26
	Water transporters	4	3	1	3.00
	Gene silencing	124	20	41	0.49
DNA replication and cell cycle	DNA repair	278	37	84	0.44
	DNA replication	113	12	38	0.32
	DNA modification	19	0	6	0
	Other DNA metabolic processes	23	4	8	0.50
	Histones	113	21	47	0.45
	Chromosome structure maintenance	82	11	29	0.38
	Cell cycle regulation	292	31	113	0.27
Development	Cell growth	154	15	72	0.21
	Tissue development	413	70	167	0.42
	Other developmental processes	164	23	53	0.43
Stress response	Response to metal	81	12	39	0.31
	Response to misfolded proteins	29	6	14	0.43
	Response to salts	89	15	36	0.42

2.4. Gene Shift in Primary Metabolism in Galls

In general, more genes in the primary pathways were up-regulated than down-regulated in gall tissues (Figure 2d). The genes encoding enzymes at different steps in the tricarboxylic acid cycle (TCA cycle) were unevenly altered in galls compared with what was observed in control leaf tissues (Figure 3). For example, the aconitate hydratase encoding gene was up-regulated strongly, but the gene encoding the succinate dehydrogenase (ubiquinone) was down-regulated in galls (Figures 3 and A1). The uneven alterations of gene expression in the TCA cycle result in the accumulation of simple sugars such as fructose, mannose, glucose, and galactose (Figure 2d). Consistent with increased accumulation of simple sugars, genes in glycolysis were also unevenly altered in galls. The gene encoding the aldehyde dehydrogenase was strongly down-regulated compared with the expression level in control leaf tissues (Figure A2). Similarly, the genes encoding fructose-bisphosphate aldolase and fructose-1,6-bisphosphatase in the pentose phosphate pathway were also down-regulated in galls, resulting in lower levels of fructose metabolism (Figure A3). The suppressed level of genes encoding the aldehyde dehydrogenase, fructose-bisphosphate aldolase, and fructose-1,6-bisphosphatase 1 suggested a lower level of sugar degradation. We also found that genes which regulated the 'starch and sucrose metabolism' and 'other glycan degradation' were more highly expressed in the gall tissues, and β -glucosidase regulated the last step in the starch and sucrose metabolism pathway by hydrolyzing the cellobiose or β -D-glucoside into D-glucose. In the same case, the glucan endo-1,3- β -D-glucosidase, which controlled the conversion of 1,3- β -glucan into D-glucose, also significantly increased in the gall tissues (Figure A4), which decompose the glycan into monosaccharide or disaccharide, thus benefitting aphids. The range of expressed difference is shown using a heatmap (Figure 2c).

Genes for photosynthesis were generally inhibited compared with control leaf tissues (Figures 2e and A5). In particular, genes encoding components in the carbon fixation were expressed at significantly lower levels (Figures 2f, 3 and A6).

There was a significant shift in the biosynthesis and degradation of amino acids. Genes involved in the biosynthesis pathways of essential amino acids, such as histidine, leucine, lysine, methionine, tryptophan, and valine, were generally up-regulated in galls. In contrast, genes involved in the biosynthesis of nonessential amino acids, such as alanine and cysteine, were generally down-regulated in galls (Figure 3, Table A7). For amino acid degradation, genes involved in the degradation of cysteine, methionine, phenylalanine, and tyrosine were down-regulated in galls, whereas genes involved in the degradation of glycine, serine, threonine, arginine, and proline were up-regulated in galls (Figure 2d, Table A8).

2.5. Gene Shift in Secondary Metabolism in Galls

The largest differences among secondary metabolic pathways between galls and control leaf tissues were found in the genes involved in phenylpropanoid pathways (Figure 3), which are involved in plant defense. There were 18 genes involved in the metabolism of various phenylpropanoids, including flavonol, isoflavonols, and anthocyanins, which were up-regulated in galls, whereas only 9 genes were down-regulated (Table A9). In addition to the shift in gene expression involved in phenylpropanoid metabolism, genes involved in terpenoid backbone and carotenoid biosynthesis were also affected (Figure 3).

2.6. Impact of Galls on the Metabolic Pathways in LNG

The trend of differences in gene expression between LNG and LWG was similar to that of differences in gene expression between galls and LWG, but at a significantly smaller scale. Only 556 unigenes showed higher transcript abundance in LNG compared with LWG. Similarly, only 781 unigenes showed lower transcript abundance (Figure 2b). Genes involved in glycan metabolism were up-regulated, but monosaccharides and disaccharides were retained (Figure 4a). Genes involved in the metabolism of selected amino acids, including tyrosine, cysteine, and methionine, were up-regulated, whereas genes involved

in the metabolism of arginine, proline, valine, tryptophan, leucine, and isoleucine were down-regulated (Figure 4a). Genes involved in fatty acid metabolic pathways and secondary metabolism were also down-regulated. Photosynthesis was slightly up-regulated (Figure 4a). The highest number of DEGs was present in plant–pathogen interaction pathways, but the number of down-regulated unigenes was close to that of up-regulated unigenes; the major changes in DEGs are listed in Table A10.

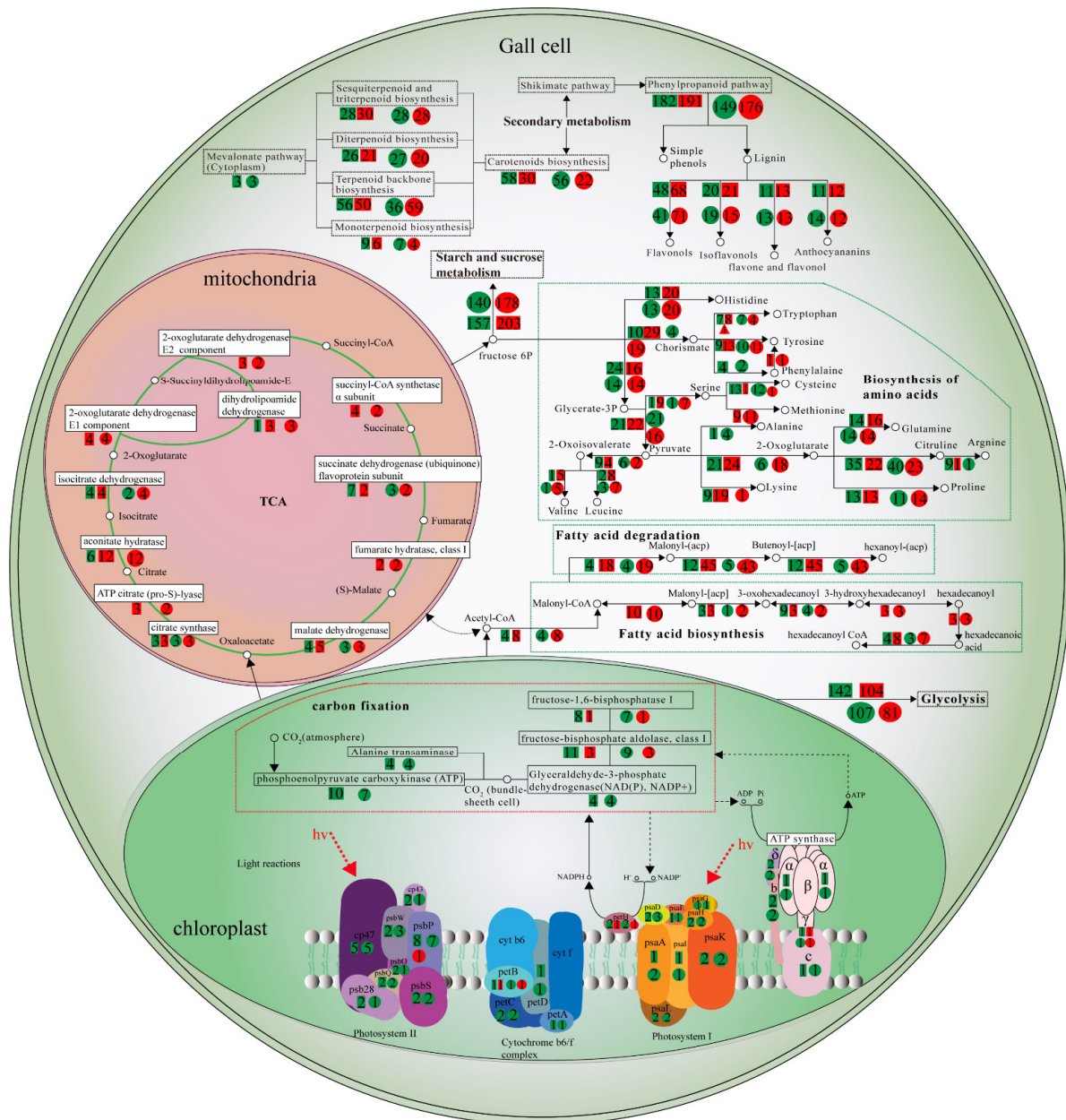


Figure 3. A model of the molecular adaptation of horned gall cells based on transcriptomic comparative analyses. Squares indicate comparison between gall vs. LWG, circles indicate comparison between gall vs. LNG, red color indicates up-regulation, and green indicates down-regulation. Arabic numerals represent the number of genes. For photosynthesis, most subpathways were down-regulated, and phosphoenolpyruvate carboxykinase was among the most down-regulated genes for carbon fixation. Although most genes involved in the TCA cycle were up-regulated, the genes encoding succinate dehydrogenase (ubiquinone) were down-regulated. Genes for biosynthesis of essential amino acids for insects were up-regulated (histidine, leucine, lysine, methionine, tryptophan, valine), except for the genes involved in the synthesis of phenylalanine and arginine. Genes for biosynthesis of nonessential amino acids (cysteine, citrulline) for insects were down-regulated. Genes involved in the production of secondary metabolites such as flavonols were generally up-regulated.

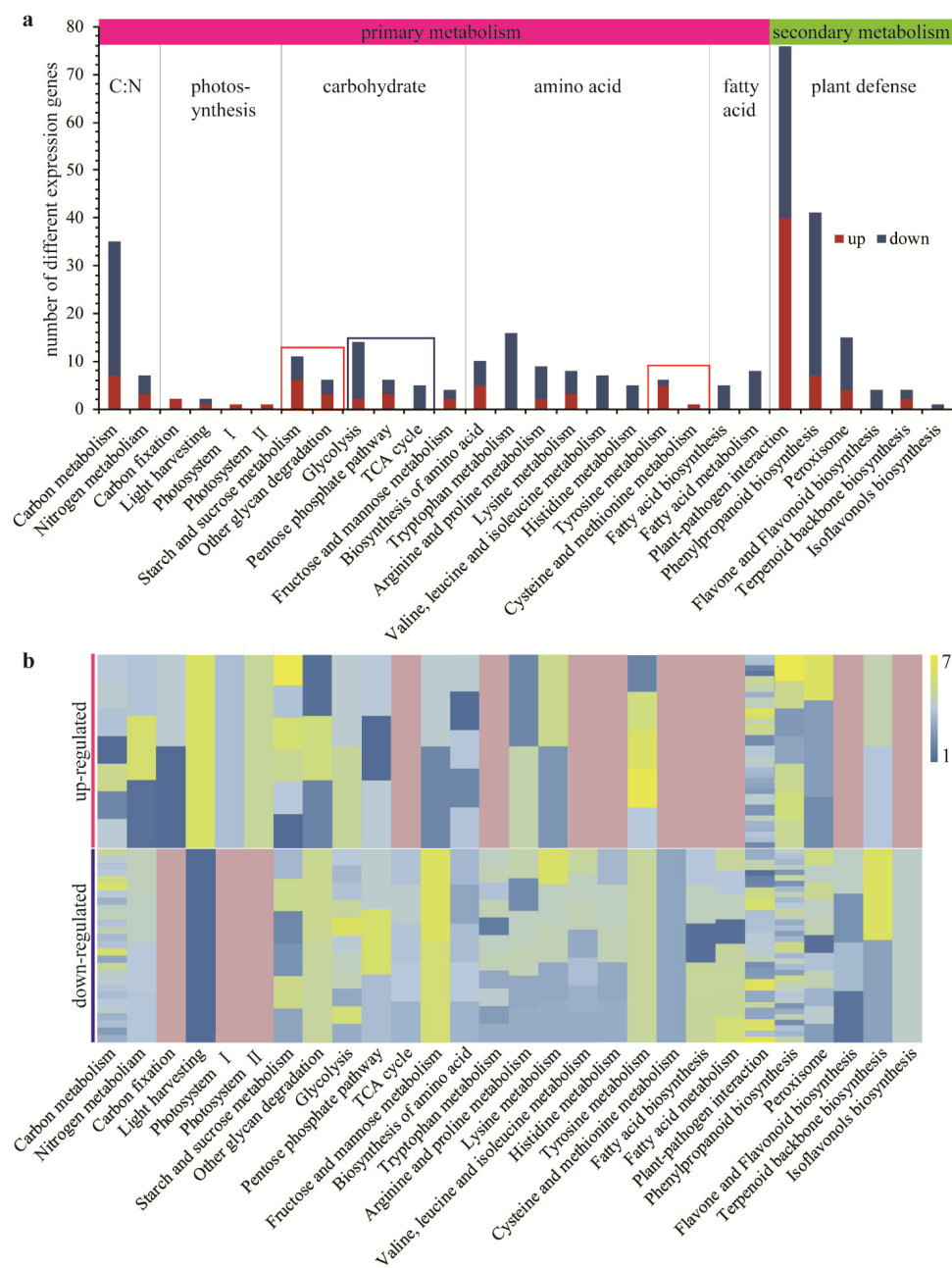


Figure 4. Pathways with DEGs between LNG vs. LWG. **(a)** DEGs in pathways for primary and secondary metabolism related to nutrient metabolism and plant defense. Genes involved in photosynthesis were up-regulated. Genes involved in metabolism of carbohydrates, most amino acids, fatty acids, and secondary metabolites (especially plant defense pathways) were down-regulated, except the plant–pathogen interaction. **(b)** Heatmap of DEGs. One box represents one gene. Pink color indicates no gene discovered. DEGs in LNG vs. LWG exhibited smaller differences in general compared with the differences between gall and leaf tissues.

2.7. Selective Expression Genes in the Gall and LNG

A more important finding was that unigenes involved in amino acid, plant development, DNA methylation, sugar pathway, lipid pathway, and plant resistance showed selective expression in LNG and the gall. (Figure 5). In the amino acid pathway, the unigene that encodes proline-rich protein 2 showed a significant difference; its FPKM in the gall was 1523.48, but it could not be detected in LNG and LWG. The unigenes that regulate proline-rich protein 4, serine carboxypeptidase, cysteine-rich receptor, and amino acid transporter showed the same tendency. The unigenes encoding glutamic acid-rich,

glutamate receptor, lysine histidine transporter, and serine/threonine-protein could be detected in the gall and LNG, but they did not express in the LWG (Figure 5a). In the plant growth pathway, three unigenes were expressed in the gall only, which regulate the MADS-box and gibberellin-regulated protein. The unigenes encoding WRKY transcription factor 33 and auxin response factor 5 were expressed in the gall and LNG (Figure 5b). The unigenes regulating the glycoside hydrolase and starch initiation protein were also expressed in the gall and LNG, but the expression level of glycoside hydrolase was lower in the LNG (Figure 5d). In the lipid pathway, the unigene that encodes lipid-transfer protein could be detected in the gall only; the unigene regulating the acetyl-CoA acyltransferase 1 showed a different expression pattern, and the expression level in the LNG was higher than that in the gall (Figure 5e). Aphids also caused changes in plant resistance. The unigene that encoded peroxidase was only expressed in the gall, and the disease resistance proteins RPM1 and RPS4 could be detected in the gall and LNG; however, the expression level of RPS4 in LNG was higher than that in the gall (Figure 5f). Notably, we found that a unigene that regulated the histone demethylase JARID1 was only expressed in the gall and LNG, and the FPKM in the gall was significantly higher than that in LNG (Figure 5c). The sequences of selective unigenes are listed in Appendix A.

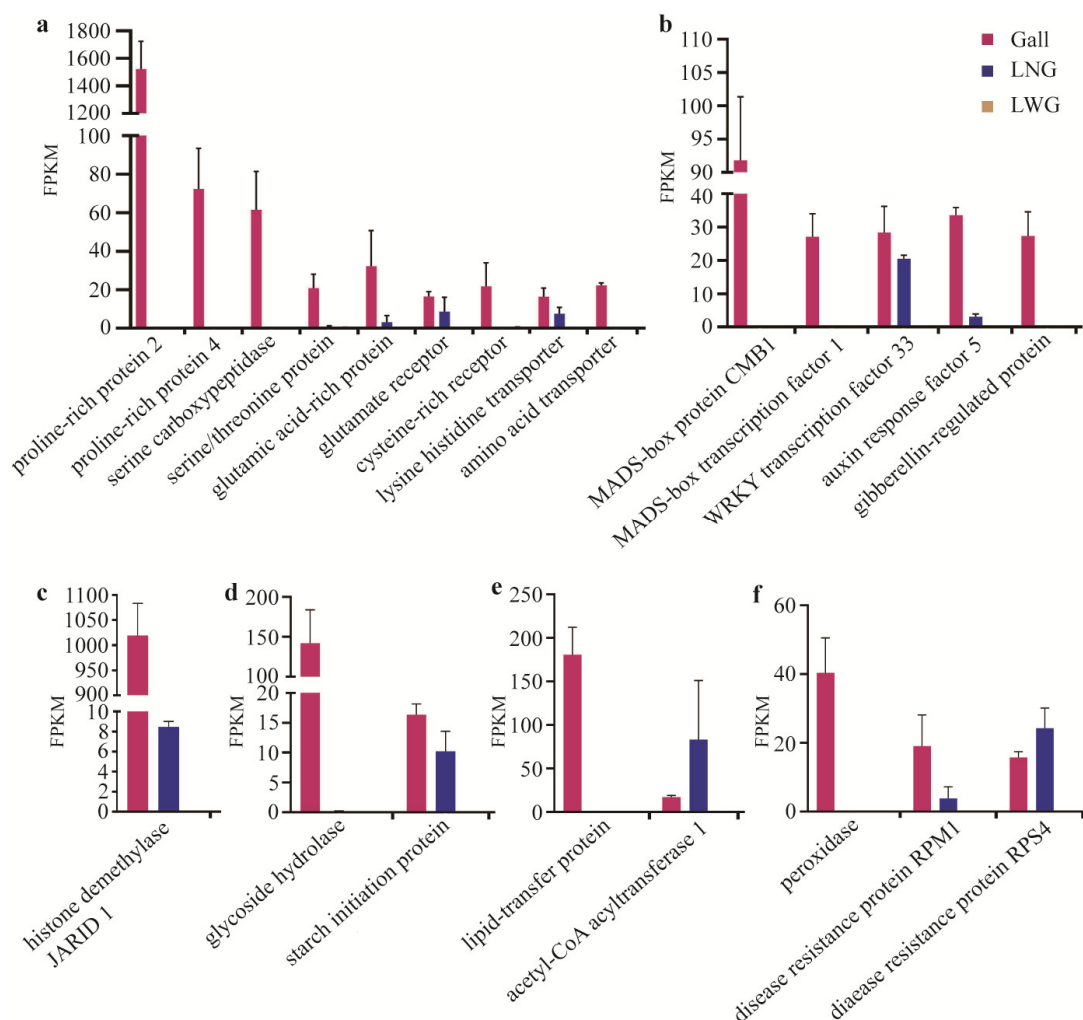


Figure 5. Selective expression genes in the gall and LNG. (a) The selective expression unigenes regulated the amino acid pathway. The unigene encoding proline-rich protein 2 showed the highest expression level in the gall. (b) The selective expression unigenes regulated the plant development. (c) The selective expression unigenes regulated the DNA methylation. (d) The selective expression unigenes regulated the sugar pathway. (e) The selective expression unigenes regulated the lipid pathway. (f) The selective expression unigenes regulated the plant resistance. Most unigenes expressed in the gall only, some unigenes expressed in the gall and LNG, and all unigenes could not be detected in the LWG.

3. Discussion

Several characteristics of horned galls on *R. chinensis* induced by *S. chinensis* are unique and notable. For example, a significant number (12 ± 6.34) of galls with large size ($86.69 \pm 13.15 \times 53.63 \pm 12.74$ mm) is exclusively localized on tiny rachis wings instead of being present on bigger leaves. A gall can carry tens of thousands of aphids, and green galls are strong candidates to perform photosynthesis [24,25]. To gain insight into these unique characteristics, we conducted comparative analyses of gene expression on the differences and similarities of metabolic pathways between galls and leaf tissues. We found several unique shifts in metabolic pathways in galls in comparison with normal leaf tissues. One of the shifts was the unbalanced changes in gene expression involved in the TCA cycle. For example, the gene encoding aconitate hydratase was up-regulated, yet the gene encoding succinate dehydrogenase was down-regulated. TCA is the central metabolic pathway of carbohydrates, lipids, and proteins [26]. The unbalanced shift of the TCA cycle might be responsible for reducing the metabolism of simple sugar and enhanced accumulation of NAD⁺/NADH. Aphids can easily utilize simple sugar and NAD⁺/NADH as nutrients. Similarly, glycolysis and pentose phosphate pathways also exhibited an unbalanced shift, favoring accumulation of simple sugar and degradation of polysaccharides and other macromolecules such as lipids and proteins. Low concentrations of glucose, fructose, sucrose, and fat were found in horned gall tissues, although biosynthesis of monosaccharides was enhanced. This is to be expected because aphids are likely to use these substances, whereas it is difficult for them to use starch directly because of their digestive system [27]. Starch is a nutrient that breaks down into glucose during the period of nutritional deficiency [28]. It is interesting to note that similar changes in gene expression were also observed in LNG compared with LWG, although the changes were at much smaller scales.

Aphids are phloem feeders; however, only a small number of amino acids in plant phloem can be obtained, meaning that aphids' demand for amino acids cannot be met [29]. Our transcriptomic analyses revealed that the galls provide solutions for this problem: the genes involved in the synthesis of essential amino acids for aphids were up-regulated in galls compared with those in normal leaves. The up- and down-regulation of selective genes are likely due to fulfilling the nutrient requirement of aphids during the long period of host–aphid coevolution. The contents of free and essential amino acids in the gall and LNG are significantly higher than those in LWG (Table A11) [30]. The molecular mechanism of this selected gene regulation in galls remains to be determined. Moreover, 99% of *S. chinensis* symbiotic bacteria are *Buchnera* spp., the main contributors of amino acids for aphids [31]. We suppose the enhanced biosynthesis pathways of essential amino acids compensate for the lack of amino acids synthesized by *Buchnera* spp.

Changes in expression levels were also found in genes involved in secondary metabolism in galls. The most interesting change in secondary metabolism was the up-regulation of most of the genes involved in phenylpropanoid metabolism. Phenylpropanoids are toxic to insects and microbes. Aphids may use phenylpropanoids as a defense chemical for potential secondary infection from microbes, whereas the aphids themselves have adapted to these toxic chemicals during the long period of coevolution. The up-regulation of phenylpropanoid genes is in contrast to most other defense genes, such as jasmonic acid and ethylene pathways, which were generally not significantly different.

A remarkable finding was that some of the selective expressed unigenes in the gall and LNG played a wide range of regulatory roles in plants, such as enhancing the enrichment and transportation of amino acids and lipids, and enhancing glycoside hydrolysis and biosynthesis of starch. These roles help to provide more suitable nutrients and standby nutrient storage. The unigenes regulating auxin and gibberellin were highly expressed in the gall, and the identified content of auxin in the gall was higher than that in normal tissues [32]. The volume of the horned gall grows rapidly with the population growth of the aphids from July to August [24]. The unigenes regulating the histone demethylase JARID1 showed the second highest FPKM (1019.54) in the gall. DNA methylation is an important

regulatory form of epigenetics and can affect a large number of biological processes, such as plants' resistance and flowering phase [33]. This indicates that the molecular regulation mechanism of the gall is more complex, and DNA methylation is an ignored factor. In general, more unigenes were selectively expressed in the gall; some of these were also expressed in LNG, but showed significantly less FPKM. We suggest that the horned gall functions as a comfortable shelter according to complex molecular regulation, and the gall affects the metabolism of nearby tissues.

Other changes in gene expression in galls include the up-regulation of genes involved in DNA synthesis, cell division, tissue development, and other structural proteins. The up-regulation of these genes may provide the basis for continuous growth of galls through the growing season (from May to October), that provides enough space for aphids. The shifts observed in primary metabolic pathways were also reported in some other gall systems [34,35]. However, a recent survey on grape leaf galls induced by *Daktulosphaira vitifoliae* suggested that genes involved in primary metabolic pathways including glycolysis and the citric acid cycle were up-regulated, resulting in a metabolic shift from autotrophic to heterotrophic [15]. Many factors can affect the functioning of plant galls, including the types of galling parasites, and the location and shape of a gall [5,36,37]. The contradictory observations among different gall systems may reflect different strategies to achieve harmonic coexistence between gall inducers and host plants.

In addition to the molecular adaption, the specialized histologic structure also plays a key role in the interaction between *R. chinensis* and *S. chinensis*. The gall wall comprises parenchyma cells, which not only store a large quantity of nutrients such as starch, but also contain a high level of tannins, which reduce the feeding times of herbivores [11]. Furthermore, the expanded xylem in the stalk can provide enough space for nutrient exchange between the aphids and their host plants. This also provides strong mechanical support via a tight connection to the host plant; a horned gall was found to weigh 10.25 ± 3.67 g and contain $19,850.11 \pm 559.43$ aphids in the latter stage of the gall development. [24]. Another remarkable characteristic of the horned gall is the presence of vast branched schizogenous ducts that are associated with the vascular bundles in the wall. These form a net that wraps the aphids. The distribution of the schizogenous ducts is regular. The average diameter of schizogenous ducts in the inner wall (3.31 ± 1.97 μm) was much smaller than those in the outer wall (6.05 ± 2.34 μm), but schizogenous ducts in the inner wall ($9.28 \pm 5.35/\text{mm}^2$) were more abundant than in the outer wall ($0.15 \pm 0.27/\text{mm}^2$) [38]. These branched structures increase the aphids' contact surface with the gall and improve the efficiency of transportation and exchange of nutrients. Thus, the stylophores gather in the schizogenous ducts.

The gall inducer can control the host plant for the inducer's benefit; thus, the gall is considered an extended phenotype of the parasite [39]. The similarity in gene expression between galls and neighboring host tissues suggests aphids induce changes in remote host tissues. However, the gall bears the majority of the stress caused by aphids by shifting its gene expression. In addition, the levels of CO_2 in galls are much (on average 8–16 times) higher than that of atmospheric CO_2 . High CO_2 within the gall could be delivered to the gall tissues and nearby leaves, and thereby enhance rates of photosynthesis [25]. Thus, feeding aphids may not have a negative effect on the trees (Figure 6).

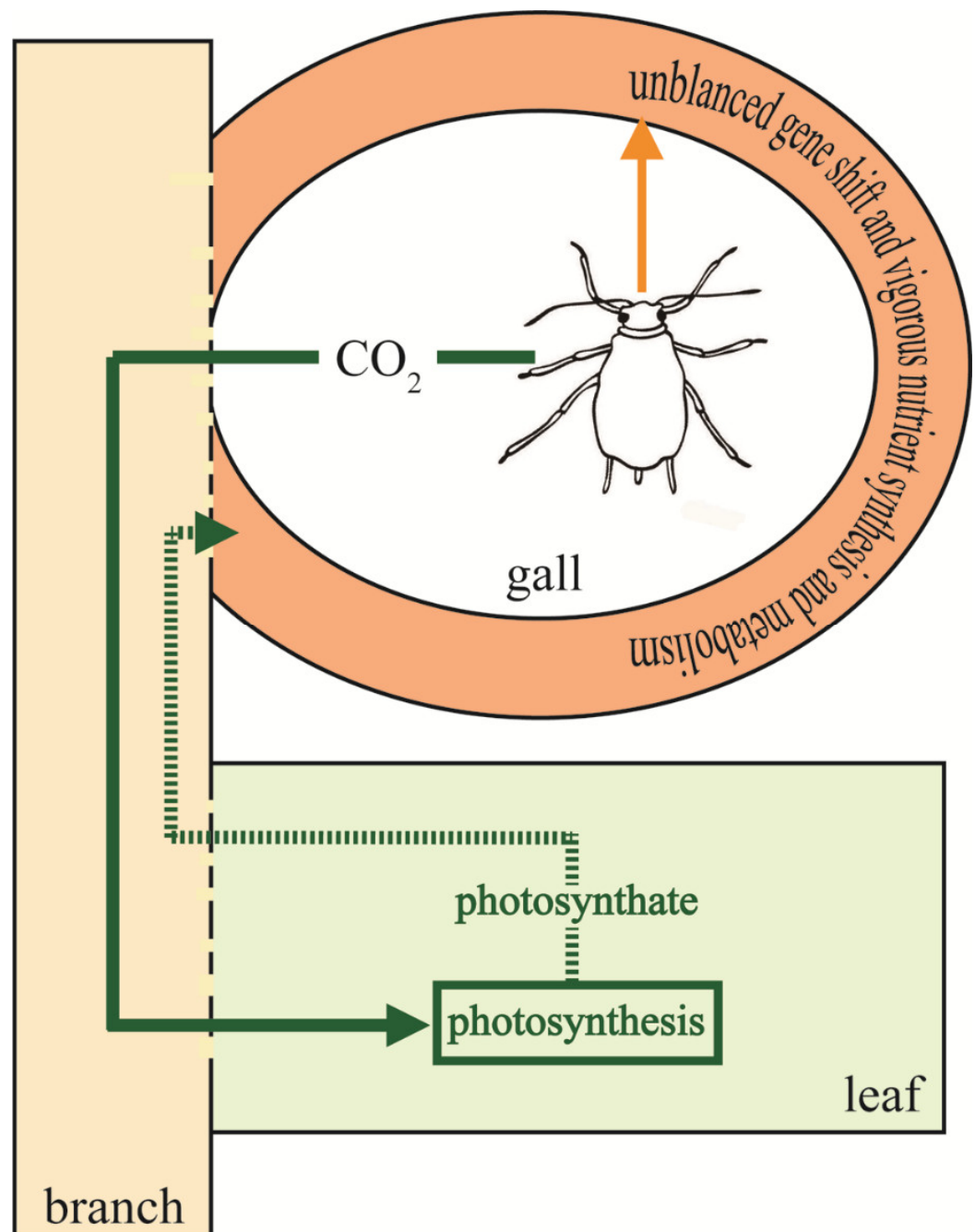


Figure 6. A model for mutualism between aphids and *R. chinensis*. Host plants provide aphids with photoassimilates, minerals, and other nutrients. The aphids can control the horned gall and the host plant for the aphids' own benefit, but the horned gall eases the direct conflict by unbalanced gene shifting and vigorous nutrient biosynthesis and metabolism. Aphids generate a high concentration of carbon dioxide, which can elevate photosynthesis of nearby leaf blades. In addition, aphids may also perform nitrogen fixation and other benefits for host plants. Due to the mutualism, leaves with multiple galls usually outgrow leaves without galls despite aphid feeding.

4. Materials and Methods

4.1. Materials

The aphids *S. chinensis* were reared on *R. chinensis* trees in the green house of the Research Institute of Resource Insects of Kunming, Yunnan province, southwest China. The samples were collected on 16 August 2019. After removing aphids from the gall tissues, the collected galls were divided into four parts. One part was frozen in liquid nitrogen and

stored at $-80\text{ }^{\circ}\text{C}$ for later isolation of RNA. Another part was used for determining the content of proteins, fats, starch, fructose, glucose, sucrose, NADP⁺, NADPH, NAD⁺, and NADH. The third part was fixed immediately in an FAA solution (5 mL formaldehyde, 5 mL acetic acid, 90 mL 70% ethyl alcohol) for 5 days and 4% glutaraldehyde for two hours, respectively. The remaining parts were cut into $5 \times 5\text{ mm}$ and placed in 50% NaOH for two days. At the same time, LNG and LWG were collected and similarly treated (Figure 7). To reduce sampling error, each sample was mixed from more than five galls or leaves from different trees. Each test had three biological replications.

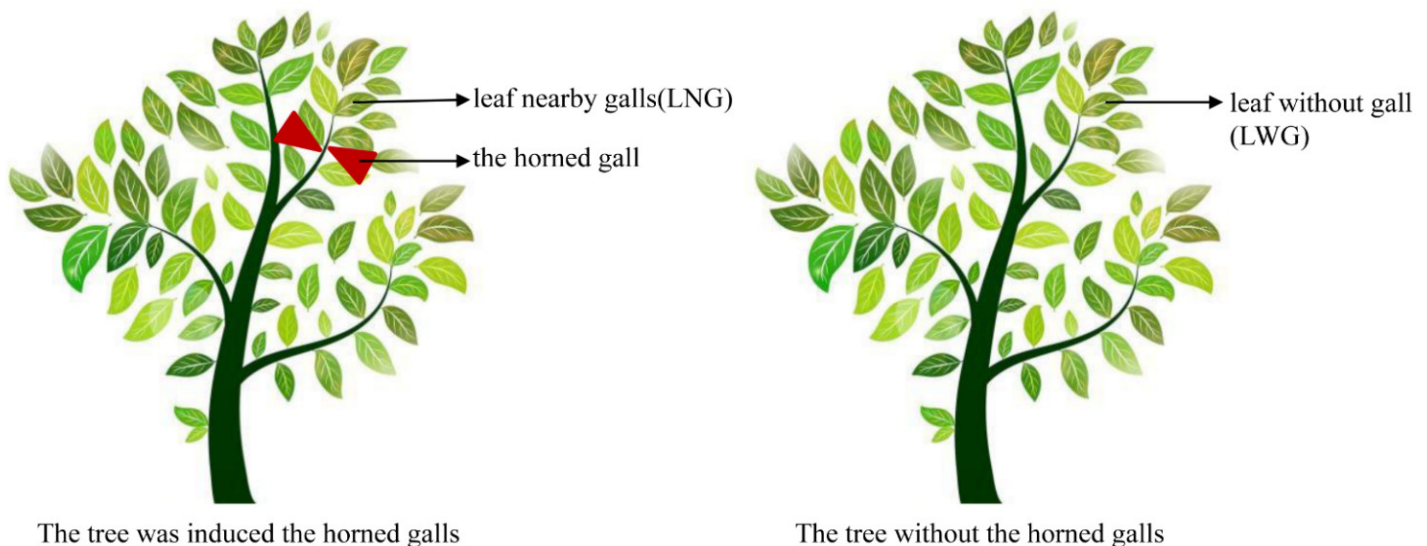


Figure 7. The samples in this study.

4.2. Tissue Anatomy

The samples in a FAA solution of the galls were cut into 2–3 mm pieces and then dehydrated in an ethanol series (70% ethyl alcohol for 30 min, 80% ethyl alcohol for 20 min, 90% ethyl alcohol for 15 min, 95% ethyl alcohol for 10 min, and 100% ethyl alcohol for 5 min). Then, ethyl alcohol was replaced by xylene and paraffin in turn. The gall samples were embedded in paraffin, 16- μm -thick sections were made using a rotary microtome (Leica RM2126RT, Solms, Hesse-Darmstadt, Germany), and the leaves were cut into 4- μm -thick sections. The sections were de-paraffinized and stained with safranin and fast green after parching.

The fixed samples in 4% glutaraldehyde were dehydrated in an ethanol series (30% ethyl alcohol for 30 min, 50% ethyl alcohol for 30 min, 70% ethyl alcohol for 30 min, 80% ethyl alcohol for 20 min, 90% ethyl alcohol for 15 min, 95% ethyl alcohol for 10 min, and 100% ethyl alcohol for 5 min) and dried in air. The dried samples were sprayed gold and observed under a SEM (Tabletop Microscope 3000, Tokyo, Japan).

The horned galls were observed via a three-dimensional microscope after treatment by 50% NaOH (MSD-VHX1000, Tokyo, Japan).

4.3. Coenzyme Measurements

The determination of coenzyme was carried out using an NAD/NADH Quantitation Colorimetric Kit (Biovision, San Francisco, CA, USA) and an NADP/NADPH Quantitation Colorimetric Kit (Biovision, San Francisco, CA, USA). The assays were performed following the instructions of the kits.

4.4. Nutrients

Protein contents were determined using the Kjeldahl nitrogen determination method (FOSS kjeltecTM 2300, Hoganas, Sweden). Fat was measured using the Soxhlet extraction

method (Rotavapor[®] R-II BUCHI, Hoganas, Sweden). Starch was determined using the enzyme hydrolysis method (Varioskan Flash, Waltham, MA, USA). Fructose, glucose, and sucrose were measured using liquid chromatography (High-Performance Liquid Chromatograph Ultimate 3000, Waltham, MA, USA).

4.5. Illumina Sequencing and Transcriptome Analysis

Total RNA was extracted from 1 mg of tissues using an RNA Extraction Kit (BioTeke Corporation, Beijing, China) according to the manufacturer's protocols. RNA purity and integrity were assessed using an RNA Nano 6000 Assay Kit (Agilent Technologies, Palo Alto, CA, USA). First strand cDNA was synthesized with random hexamers as primers and mRNA fragments as templates. Double-stranded cDNA was synthesized and purified using a QiaQuick PCR Extraction kit (QIAGEN, Dusseldorf, North Rhine-Westphalia, Germany). End repair and the addition of adenines were carried out in the EB buffer. Sequencing adaptors were ligated to fragments, and the resulting fragments were purified through agarose gel electrophoresis and enriched by PCR amplification. Sequencing libraries were generated using a Next Ultra Directional RNA Library Prep Kit from Illumina (New England Biolabs, Beijing, China). After cluster generation, the libraries were sequenced on an Illumina HiSeq 2000 platform (BGI, Shenzhen, Guangdong, China), and paired-end reads were generated. Finally, products were purified with the AMPure XP system (Beckman Coulter, Brea, CA, USA), and library quality was confirmed on an Agilent 2100 Bioanalyzer (Agilent Technologies, Palo Alto, CA, USA).

Reads with adaptors or more than 10% unknown bases, in addition to other low-quality reads, were removed prior to data analysis. Transcriptome assembly was accomplished using Trinity with default parameters [40]. The sequences were assessed by read quality, statistics of alignment analysis, sequencing saturation analysis, distribution of reads on the reference gene, and distribution of reads on the reference genome.

4.6. Gene Annotation

Gene function of all assembled unigenes was annotated based on the Nr, Nt, Swiss-Prot, KEGG, COG, and GO databases.

4.7. Differentially Expressed Genes (DEGs)

Based on the gene expression level (FPKM), we identified the DEGs among samples, and the DEGs of gall vs. LWG, gall vs. LNG, and LNG vs. LWG were calculated by \log_2 fold change (Gall/LWG, Gall/LNG, and LNG/LWG), respectively. Fold change of >1 indicated up-regulation, whereas a negative fold change indicated down-regulation.

5. Conclusions

Our study revealed extensive gene shifts in primary and secondary metabolic pathways in *R. chinensis* horned galls induced by the aphid *S. chinensis*. Most shifts in gene expression appeared to be driven by adaptation to satisfy nutrient needs of aphids. The complex metabolism of photosynthesis in gall tissues is different from that of normal tissues. Genes that accommodate the aphids were selectively expressed in the gall and LNG, and indicate DNA methylation is an ignored regulatory factor in the gall. Furthermore, the horned galls have specialized histological structures such as branched schizogenous ducts and expanded xylem. Due to its molecular foundation and histological adaption, the horned gall is a medium that eases direct conflict between the aphids and the host plant, so the normal physiological state of *R. chinensis* can be maintained. As a result, galling aphids have formed a relatively harmonic co-existence with their host plants via partially self-supporting galls.

Author Contributions: H.C. and X.C. designed and led the project. Transcriptome data generation and samples collection were performed by Y.C., J.L. and S.S., Z.Y. took the photo. Q.L. undertook the paraffin section and analyzed the transcriptome data. The first draft of the manuscript was written

by Q.L. and M.-S.C., N.H.B. revised the paper. All authors have read and agreed to the published version of the manuscript.

Funding: This research was funded by the Fundamental Research Funds of CAF (CAFYBB2020QA003), the Program of Innovative Team of Yunnan Province (202005AE160011), and Applied Basic Research Foundation of Yunnan Province (2019FD027).

Institutional Review Board Statement: Not applicable.

Informed Consent Statement: Not applicable.

Data Availability Statement: The data that support the findings of this study are openly available in the NCBI Sequence Read Archive (SRA) under projects PRJNA631065 (<https://www.ncbi.nlm.nih.gov/bioproject/PRJNA631065>). Access worked from 7 May 2020).

Conflicts of Interest: The authors declare no conflict of interest.

Appendix A

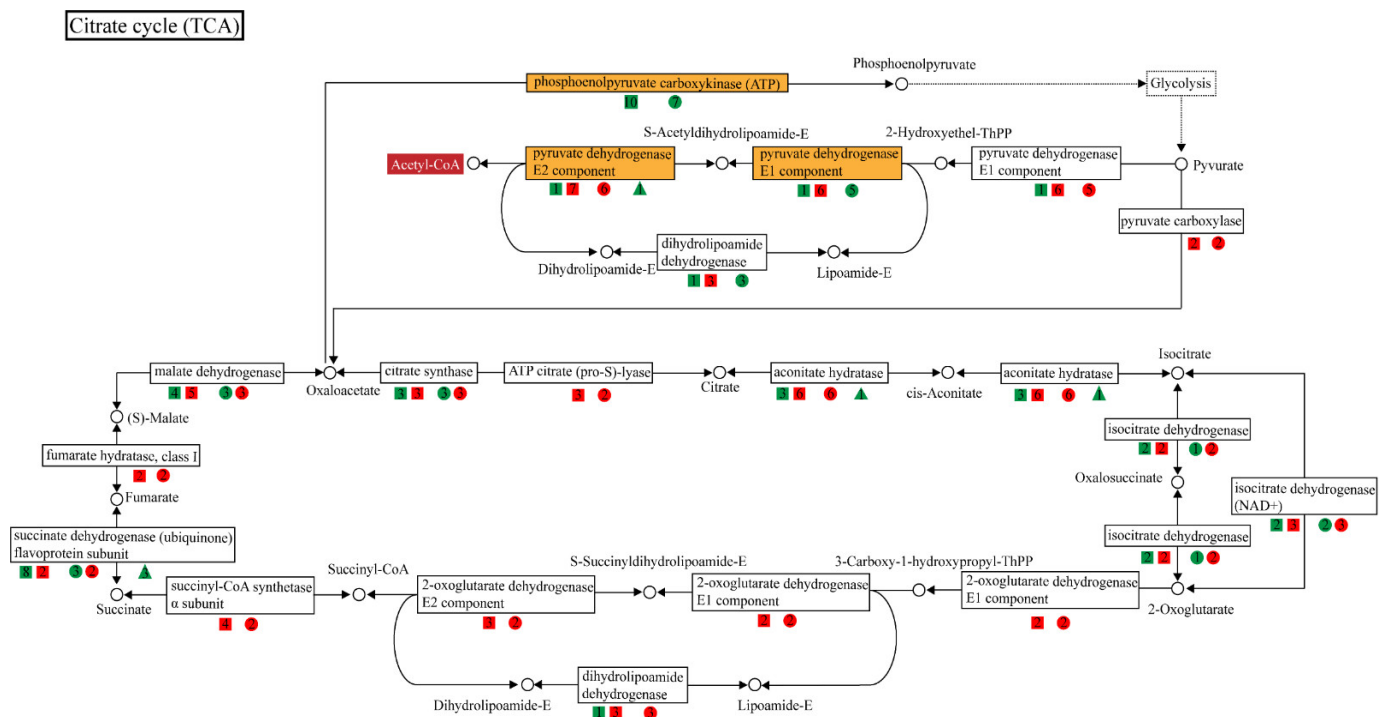


Figure A1. DEGs in the TCA cycle. Squares represent DEGs based on the comparison between gall vs. LWG; circles represent DEGs based on the comparison between gall vs. LNG; triangles represent DEGs based on the comparison between LNG vs. LWG. Red color indicates up-regulation and green color indicates down-regulation. The numbers within shaded shapes indicate the number of genes. There were 52 genes up-regulated and 34 genes down-regulated based on the comparison between gall vs. LWG, 44 genes up-regulated and 19 genes down-regulated based on the comparison between gall vs. LNG, and 5 genes down-regulated based on the comparison between LNG vs. LWG. The gene encoding aconitate hydratase was strongly up-regulated, but the gene encoding succinate dehydrogenase (ubiquinone) flavoprotein subunit was down-regulated in galls.

Glycolysis

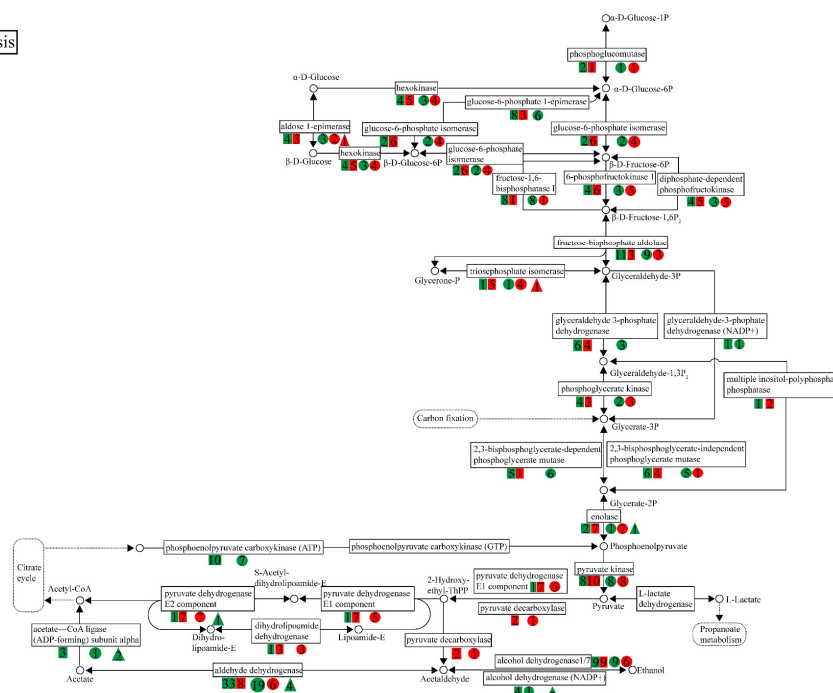


Figure A2. DEGs in glycolysis. Squares represent DEGs based on the comparison between gall vs. LWG; circles represent DEGs based on the comparison between gall vs. LNG; triangles represent DEGs based on the comparison between LNG vs. LWG. Red color indicates up-regulation and green color indicates down-regulation. The numbers within shaded shapes indicate the number of genes. There were 104 genes up-regulated and 142 genes down-regulated based on the comparison between gall vs. LWG, 81 genes up-regulated and 107 genes down-regulated based on the comparison between gall vs. LNG, two genes up-regulated and 11 genes down-regulated based on the comparison between LNG vs. LWG. In general, genes involved in glycolysis were down-regulated.

Pentose phosphate pathway

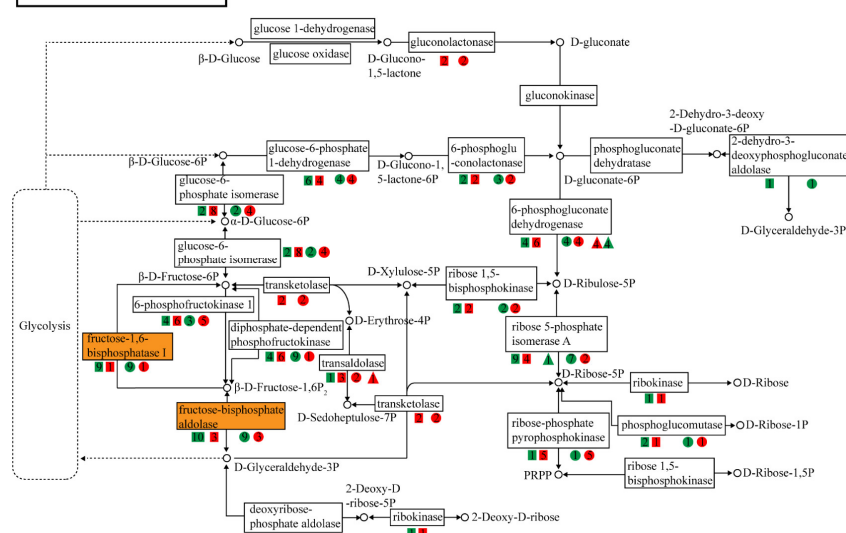


Figure A3. DEGs in pentose phosphate pathway. Squares represent DEGs based on the comparison between gall vs. LWG; circles represent DEGs based on the comparison between gall vs. LNG; triangles represent DEGs based on the comparison between LNG vs. LWG. Red color indicates up-regulation and green color indicates down-regulation. The numbers within shaded shapes indicate the number of genes. There were 48 genes up-regulated and 53 genes down-regulated based on the comparison between gall vs. LWG, 40 genes up-regulated and 44 genes down-regulated based on the comparison between gall vs. LNG, three genes up-regulated and three genes down-regulated based on the comparison between LNG vs. LWG. The genes encoding fructose-bisphosphate aldolase and fructose-1,6-bisphosphate I were down-regulated.

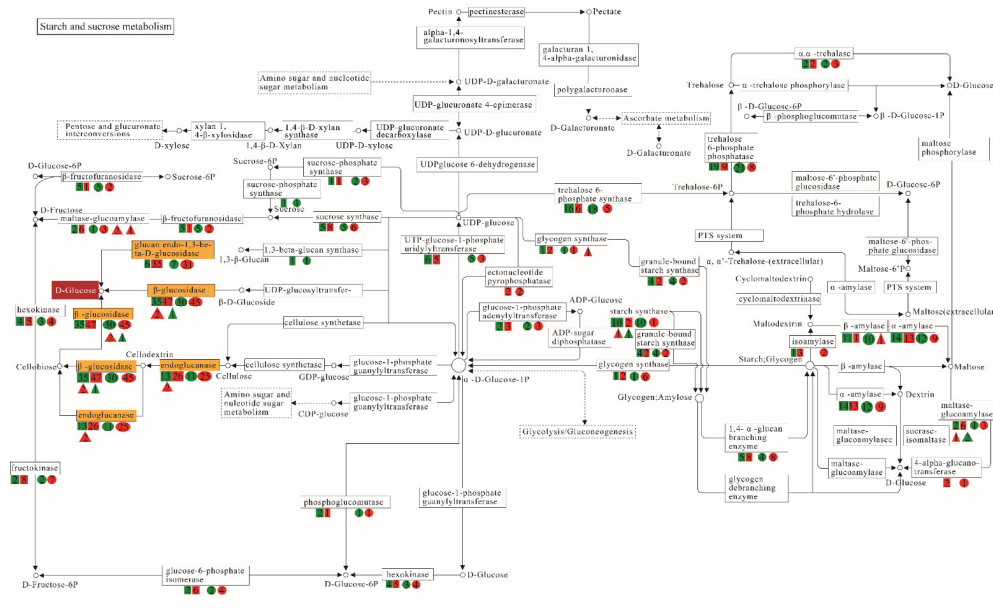


Figure A4. DEGs in starch and sucrose metabolism. Squares indicate DEGs based on the comparison between gall vs. LWG; circles indicate DEGs based on the comparison between gall vs. LNG; triangles indicate DEGs based on the comparison between LNG vs. LWG. Red color represents up-regulation and green color represents down-regulation. The numbers within shaded shapes indicate the number of genes. There were 203 genes up-regulated and 157 genes down-regulated based on the comparison between gall vs. LWG; 178 genes up-regulated and 140 genes down-regulated based on the comparison between gall vs. LNG; and 10 genes up-regulated and four genes down-regulated based on the comparison between LNG vs. LWG. DEGs encode β -glucosidase (47 genes up-regulated and 35 genes down-regulated in LWG vs. gall) and the glucan endo-1,3- β -D-glucosidase, both of which participate in D-glucose synthesis.

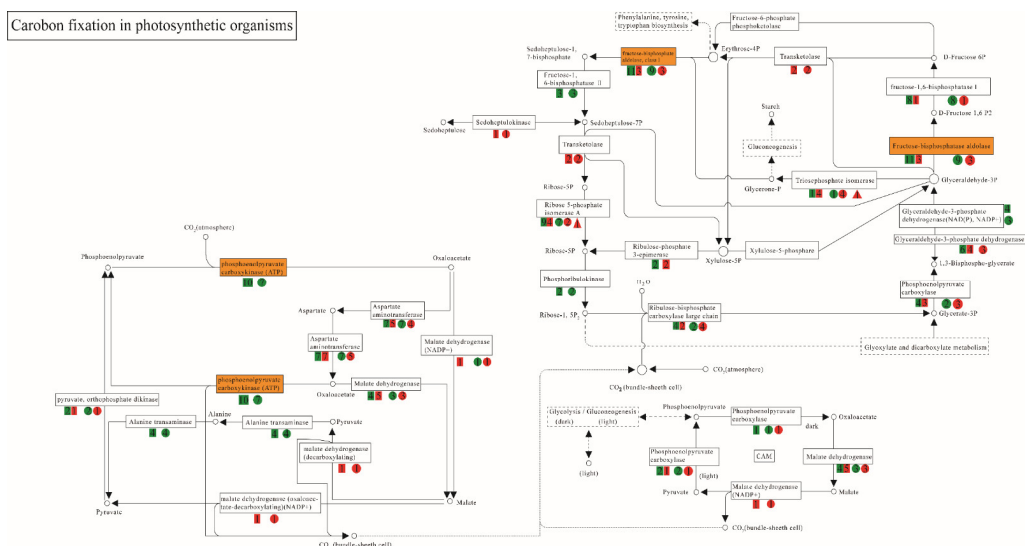
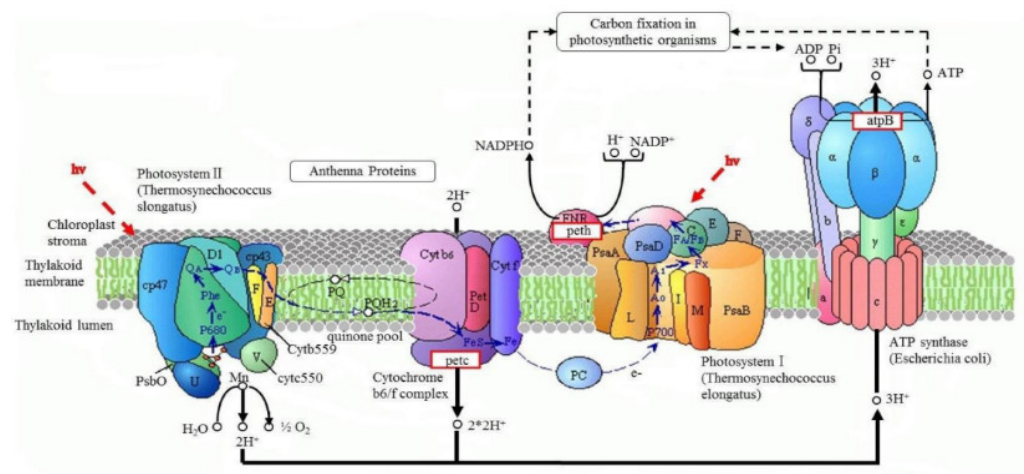
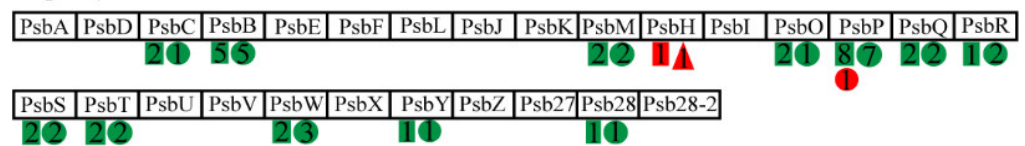


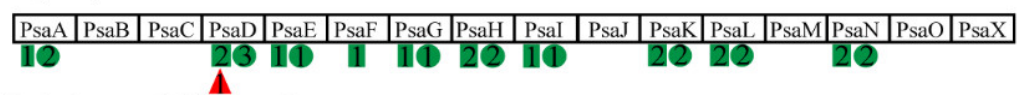
Figure A5. DEGs in carbon fixation. Squares indicate gall vs. LWG.; circles indicate gall vs. LNG; triangles indicate LNG vs. LWG. Red color represents up-regulation and green color represents down-regulation. The numbers within shaded shapes indicate the number of genes. There were 51 genes up-regulated and 100 genes down-regulated based on the comparison between gall vs. LWG, 46 genes up-regulated and 81 genes down-regulated based on the comparison between gall vs. LNG, two genes up-regulated based on the comparison between LNG vs. LWG. The genes encoding the first enzyme (phosphoenolpyruvate carboxykinase) in the reaction of transporting CO₂ into cells and the enzyme fructose-bisphosphate aldolase were strongly down-regulated.



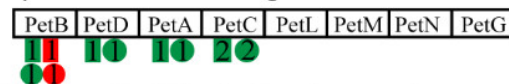
Photosystem II



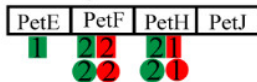
Photosystem I



Cytochrome b6/f complex



Photosynthetic electron transport



F-type ATPase



Figure A6. DEGs in photosystem. Squares indicate gall vs. LWG; circles indicate gall vs. LNG; triangles indicate LNG vs. LWG. Red color represents up-regulation and green color represents down-regulation. The numbers within shaded shapes indicate the number of genes. There were six genes up-regulated and 62 genes down-regulated based on the comparison between gall vs. LWG, six genes up-regulated and 61 genes down-regulated based on the comparison between gall vs. LNG, two genes up-regulated based on the comparison between LNG vs. LWG. Most genes involved in photosynthesis were down-regulated in galls.

Table A1. Statistics of transcriptome.

	Sample	Total Number	Total Length (bp)	Mean Length (bp)	N50	GC%
Unigene	Rhuscm	112,543	127,567,799	1133	2061	40.34

Sample: Sample name; Total Number: The total number of transcripts; Total Length: The read length of transcripts; Mean Length: The average length of transcripts; N50: a weighted median statistic that 50% of the total length is contained in Unigenes that are equal to or larger than this value; GC(%): the percentage of G and C bases in all transcripts.

Table A2. Quality evaluation of clean reads.

Samples	Total Raw Reads (Mb)	Total Clean Reads (Mb)	Total Clean Bases (Gb)	Q20 Percentage (%)	Q30 Percentage (%)	Clean Reads Ratio (%)
Gall-1	45.72	44.23	6.63	98.27	95.56	96.73
Gall-2	45.72	44.11	6.62	98.27	95.56	96.47
Gall-3	45.72	44.07	6.61	98.25	95.51	96.39
LWG-1	47.36	45.53	6.84	98.15	95.28	96.15
LWG-2	47.36	45.60	6.83	98.19	95.38	96.28
LWG-3	47.36	45.56	6.84	98.22	95.44	96.21
LNG-1	47.36	45.61	6.84	98.29	95.60	96.31
LNG-2	45.72	44.04	6.61	98.32	95.69	96.33
LNG-3	47.36	45.61	6.84	98.29	95.61	96.31

Sample: Sample name; Total Raw Reads(Mb): The reads amount before filtering; Total Clean Reads(Mb): The reads amount after filtering; Total Clean Bases(Gb): The total base amount after filtering; Clean Reads Q20(%): The rate of bases which quality is greater than 20 value in clean reads; Clean Reads Q30(%): The rate of bases which quality is greater than 30 value in clean reads; Clean Reads Ratio(%): The ratio of the amount of clean reads.

Table A3. Quality evaluation of transcripts.

Samples	Total Number	Total Length	Mean Length	N50	N70	N90	GC (%)
Gall-1	59,801	52,964,643	885	1663	996	318	41.02
Gall-2	66,917	57,745,662	862	1603	938	313	41.19
Gall-3	57,263	48,501,165	846	1552	915	308	41.72
LWG-1	82,726	60,330,352	729	1435	717	258	40.20
LWG-2	63,813	54,324,268	851	1598	942	305	40.77
LWG-3	68,304	55,058,251	806	1545	875	282	40.41
LNG-1	59,628	51,521,169	864	1602	956	311	41.05
LNG-2	59,609	53,137,603	891	1646	1000	326	40.52
LNG-3	59,127	52,809,348	893	1621	995	329	40.45

Sample: Sample name; Total Number: The total number of transcripts; Total Length: The read length of transcripts; Mean Length: The average length of transcripts; N50: The N50 length is used to determine the assembly continuity, the higher the better, N50 is a weighted median statistic that 50% of the total length is contained in Unigenes that are equal to or larger than this value; N70: Similar to N50; N90: Similar to N50; GC(%): the percentage of G and C bases in all transcripts.

Table A4. Quality evaluation of unigenes.

Samples	Total Number	Total Length	Mean Length	N50	N70	N90	GC(%)
Gall-1	42,432	45,357,023	1068	1810	1190	422	41.16
Gall-2	48,483	49,794,838	1027	1745	1118	403	41.33
Gall-3	41,018	41,199,383	1004	1703	1093	389	41.84
LWG-1	54,078	49,698,140	919	1656	1002	332	40.52
LWG-2	43,523	45,592,506	1047	1760	1152	421	40.89
LWG-3	46,052	46,151,536	1002	1727	1117	383	40.64
LNG-1	41,269	43,554,246	1055	1758	1162	428	40.14
LNG-2	41,022	44,757,790	1091	1796	1195	457	40.68
LNG-3	41,402	44,364,938	1071	1757	1173	447	40.62

Sample: Sample name; Total Number: The total number of Unigenes; Total Length: The read length of Unigenes; Mean Length: The average length of Unigenes; N50: The N50 length is used to determine the assembly continuity, the higher the better. N50 is a weighted median statistic that 50% of the total length is contained in transcripts that are equal to or larger than this value.; N70: Similar to N50; N90: Similar to N50; GC(%): the percentage of G and C bases in all Unigenes.

Table A5. Annotation results in different databases.

Database	Numbers of Unigene	Percent (%)
Total	112,543	100
Nr	66,783	59.34
Nt	52,701	46.83
Swiss-Prot	45,341	40.29
KEGG	51,648	45.89
KOG	55,832	49.61
Interpro	60,048	53.36
GO	36,323	32.27
Intersection	20,113	17.87
Overall	76,949	68.37

Intersection: The number of Unigenes which annotated by all the 7 functional databases; Overall: The number of Unigenes which annotated by any of the 7 functional databases. *Cut-off E-value $\leq 10^{-5}$.

Table A6. The top 10 enzymes with the largest differences in seven pathways for which gene shifts were significant.

Functional Category/Subcategory	Down-Regulated	UpRegulated
Pentose-phosphate shunt	thiamine biosynthesis protein ThiC GTP-binding protein LepA ATP-binding protein involved in chromosome partitioning plastid-lipid-associated protein 12 peptidylprolyl isomerase ATP-binding protein involved in chromosome partitioning phospholipase D ATP-dependent RNA helicase DDX56/DBP9 D-threo-aldose 1-dehydrogenase tRNA (cytosine38-C5)-methyltransferase	glucose-6-phosphate 1-dehydrogenase pyridoxine biosynthesis protein acetyltransferase NSI-like transaldolase oxidoreductase YkwC-like
Vitamin	farnesol kinase acyl-activating enzyme 14 naphthoate synthase MSBQ methyltransferase tyrosine aminotransferase glutamine amidotransferase 6-phosphogluconolactonase	vitamin E vitamin B
pentose phosphate pathway	myo-inositol-1(or 4)-monophosphatase ATP synthase protein I transcription initiation factor TFIIIF subunit alpha	ferritin heavy chain adenylylsulfate kinase
Iron and sulfate metabolism	polyadenylate-binding protein cysteine desulfurase prolyl-tRNA synthetase bis(5'-adenosyl)-triphosphatase (E)-4-hydroxy-3-methylbut-2-enyl-diphosphate synthase BoLA protein selenocysteine lyase	
small molecule metabolism	carbonic anhydrase CUG-BP- and ETR3-like factor metal ion binding protein	electron transfer flavoprotein beta subunit 3-oxoacyl-[acyl-carrier protein] reductase betaine-aldehyde dehydrogenase COQ10 B, mitochondrial precursor 4-hydroxybenzoate hexaprenyltransferase aldehyde dehydrogenase (NAD+) alcohol dehydrogenase omega-hydroxypalmitate O-feruloyl transferase AdoMet-dependent rRNA methyltransferase SPB1 F-box protein 3

Table A6. Cont.

Functional Category/Subcategory	Down-Regulated	UpRegulated
Disease resistance proteins	Disease resistance protein RPM1 MLO-like protein 4-like disease resistance protein At4g27190-like Disease resistance protein RFL1 disease resistance protein At4g27190-like Disease resistance protein RPP13 disease resistance protein At1g61300-like Disease resistance protein RPS2 MLO-like protein 13-like disease resistance protein At4g27190-like	mlo protein disease resistance protein RPM1 disease resistance protein RPS5
ATP-dependent proteases	ATP-dependent metalloprotease ATP-dependent Clp protease cell division protease FtsH ATP-dependent Clp protease adaptor protein ClpS	ATP-dependent RNA helicase DHX8/PRP22 AFG3 family protein
Cysteine proteases	cathepsin L cysteine protease inhibitor cathepsin H bark storage protein A-like nudix hydrolase 8-like cytosolic purine 5'-nucleotidase nudix hydrolase 10 3-5 exonuclease cytosolic purine 5'-nucleotidase	cysteine protease
Metabolism	nudix hydrolase 20, chloroplastic-like nitrilase homolog 1-like adenine phosphoribosyltransferase dihydropyrimidinase callose synthase centromeric protein E dynein light chain LC6 nucleoprotein TPR actin 1 microtubule-associated protein 70-5-like	nucleoside-diphosphate kinase ribonuclease Z thyroid adenoma-associated protein homolog uridine monophosphate synthetase GDPmannose 4,6-dehydratase ubiquitin carboxyl-terminal hydrolase 36/42 ribose-phosphate pyrophosphokinase elongation factor Tu ribonucleoside-diphosphate reductase subunit M1 adenosine kinase
Structure	Rho GDP-dissociation inhibitor kinesin family member C1 dynein light chain LC8-type microtubule organization protein tubulin gamma large subunit ribosomal protein L2 small subunit ribosomal protein S16e small subunit ribosomal protein S1 large subunit ribosomal protein L1 small subunit ribosomal protein S18 large subunit ribosomal protein L24	tubulin beta microfibrillar-associated protein 1 tubulin gamma Kinesin family member 11 nuclear pore complex protein Nup62 gelsolin nuclear pore complex protein Nup62 kinesin family member 15 kinesin family member 22 kinesin family member 18/19 exportin-1
Ribosomal proteins	50S ribosomal protein 6 30S ribosomal protein S31 large subunit ribosomal protein L15 small subunit ribosomal protein S9 xial regulator YABBY 5 threonine-protein kinase/endoribonuclease peptide chain release factor 1 auxin-responsive protein peptide chain release factor 2 nucleic acid binding protein	large subunit ribosomal protein LP1 small subunit ribosomal protein S25e small subunit ribosomal protein S6e large subunit ribosomal protein L31e large subunit ribosomal protein L27Ae large subunit ribosomal protein LP0 large subunit ribosomal protein L37Ae large subunit ribosomal protein L13e small subunit ribosomal protein S14e small subunit ribosomal protein S21e

Table A6. Cont.

Functional Category/Subcategory		Down-Regulated	UpRegulated
	Translation	peptidyl-tRNA hydrolase translation initiation factor e endoribonuclease	ATP-dependent RNA helicase DDX6/DHH1 auxin-responsive protein translation initiation factor 3 subunit K
		protein TIF31 eukaryotic translation initiation factor 3 subunit farnesol dehydrogenase translation initiation factor 5A transcription initiation factor TFIIE subunit beta translation initiation factor eIF-2B subunit beta translation initiation factor IF-1 translation initiation factor 1 KIAA0664 homolog translation initiation factor IF-3	translation initiation factor 5A translation initiation factor 4A translation initiation factor 2 subunit 3 translation initiation factor 4E translation initiation factor eIF-2B subunit gamma protein TIF31 translation initiation factor 3 subunit I ATP-dependent RNA helicase translation initiation factor 3 subunit D translation initiation factor 2 subunit 1
	Initiation		
	Elongation	elongation factor G elongation factor P	elongation factor 2 elongation factor 1-alpha elongation factor 1-beta elongation factor Ts elongation factor G elongation factor P
	Others	small subunit ribosomal protein S6 NAD(P)H-quinone oxidoreductase subunit 2 thylakoid membrane organization large subunit ribosomal protein L27 large subunit ribosomal protein L17 large subunit ribosomal protein L9 large subunit ribosomal protein L7/L12 large subunit ribosomal protein L18 small subunit ribosomal protein S13 Mitochondrial protein	small subunit ribosomal protein S24e large subunit ribosomal protein L10Ae small subunit ribosomal protein S4e small subunit ribosomal protein S23e large subunit ribosomal protein L19e large subunit ribosomal protein L17e large subunit ribosomal protein L8e large subunit ribosomal protein L39e small subunit ribosomal protein S2e small subunit ribosomal protein S15Ae
	Protein myristoylation	U6 small nuclear ribonucleoprotein PRP4 glycylpeptide N-tetradecanoyltransferase protein N-terminal asparagine amidohydrolase acylaminoacyl-peptidase kinesin family member C1	phosphoethanolamine N-methyltransferase heat shock protein 90kDa beta glycylpeptide N-tetradecanoyltransferase vacuolar protein 8 importin alpha E3 ubiquitin-protein ligase TRIP12 stromal membrane-associated protein solute carrier family 44 auxin response factor
Transport	Lipid and fatty acid transport	Cell wall-associated hydrolase phospholipid-translocating ATPase non-specific lipid-transfer protein 1-like lipid transfer protein precursor	lipid binding protein non-specific lipid-transfer protein diazepam-binding inhibitor non-specific lipid-transfer protein 2-like phospholipid-translocating ATPase uncharacterized GPI-anchored protein Atlg27950 phospholipid-translocating ATPase uncharacterized protein LOC100305635 precursor tRNA wybutosine-synthesizing protein 3 Niemann-Pick C1 protein

Table A6. Cont.

Functional Category/Subcategory	Down-Regulated	UpRegulated
vesicle-mediated and intracellular transport	<p>syntaxin-41 charged multivesicular body protein 3 Arf/Sar family prolyl oligopeptidase exocyst complex component 7 ADP-ribosylation factor-like protein 5 phospholipase D vesicle-mediated transport FK506-binding nuclear protein transforming growth factor-beta receptor-associated protein 1-like</p>	<p>synaptosomal-associated protein FK506-binding nuclear protein coatamer protein complex syntaxin-binding protein 1 clathrin heavy chain FK506-binding nuclear protein syntaxin 5 ESCRT-II complex subunit VPS36 oxidation resistance protein 1-like Prenylated Rab acceptor protein</p>
Water transporters	<p>solute carrier family 50 aquaporin NIP aquaporin TIP</p>	<p>aquaporin PIP aquaporin TIP aquaporin-4 aquaporin NIP 3'-phosphoadenosine 5'-phosphosulfate synthase protein brassinosteroid insensitive 2 aquaporin SIP solute carrier family 50 exocyst complex component 7</p>
Gene silencing	<p>arginine and glutamate-rich protein 1 RING finger and CHY zinc finger domain-containing protein 1 THO complex subunit 3 symplekin fused signal recognition particle receptor protein MPE1 fused signal recognition particle receptor UDP-N-acetylglucosamine pyrophosphorylase RNA-binding protein 5/10 kinesin family member C2/C3</p>	<p>interleukin-1 receptor-associated kinase 4 structural maintenance of chromosome 4 kinesin family member 15 auxin response factor cell division cycle 20-like protein 1 chromatin assembly factor 1 subunit A copper chaperone SNF-related matrix-associated actin-dependent regulator of chromatin subfamily A member 5 LRR receptor-like serine/threonine-protein kinase FLS2</p>
DNA replication and cell cycle	<p>DNA repair</p> <p>deoxyribodipyrimidine photo-lyase deoxyribonuclease V riboflavin kinase UDP-glucosyl transferase 73C Bola protein heat shock protein HspQ peptide-N4-(N-acetyl-beta- glucosaminy)asparagine amidase DNA ligase 4 DNA mismatch repair protein MutS2 DNA mismatch repair protein MutS2</p>	<p>nucleosome assembly protein 1-like 1 dUTP pyrophosphatase ATP-dependent RNA helicase DDX31/DBP7 peptide-N4-(N-acetyl-beta- glucosaminy)asparagine amidase DNA cross-link repair 1B protein DNA repair protein RAD51 deoxyribodipyrimidine photo-lyase DNA-3-methyladenine glycosylase kinetochore protein Spc25 DNA-3-methyladenine glycosylase II</p>

Table A6. Cont.

Functional Category/Subcategory	Down-Regulated	UpRegulated
DNA replication	DNA polymerase eta subunit leucine-rich repeat-containing protein 40-like histone-binding protein RBBP4 DNA primase small subunit LRR receptor-like serine replication factor C subunit 3/5 DNA cross-link repair 1A protein adenosylmethionine-8-amino-7-oxononanoate aminotransferase E3 ubiquitin-protein ligase UBR7	GIN5 complex subunit 3 phospholipase D high mobility group protein B1 histone-binding protein RBBP4 DNA polymerase eta subunit minichromosome maintenance protein 7 DNA polymerase alpha subunit A DNA polymerase alpha subunit A thymidine kinase DNA primase large subunit
DNA modification		DNA (cytosine-5-)-methyltransferase F-box protein, helicase, 18
Other DNA metabolic processes	putative holliday junction resolvase	translation initiation factor 3 subunit M serine/arginine repetitive matrix protein 1 ATP-dependent DNA helicase RecG
Histones	enhancer of zeste ATP-binding cassette, subfamily F, member 2 histone-lysine N-methyltransferase SETD1 histone deacetylase 6/10 histone H1/5 chromodomain-helicase-DNA-binding protein 4 [ribulose-bisphosphate carboxylase]-lysine N-methyltransferase SAGA-associated factor 29 enhancer of zeste histone acetyltransferase	histone H2B histone H2A nuclear transcription Y subunit beta histone-lysine N-methyltransferase SETD1 chromodomain-helicase-DNA-binding protein 4 enhancer of zeste histone H3 U4/U6.U5 tri-snRNP-associated protein 1 beta-1,3-galactosyltransferase nucleophosmin 1
Chromasome structure maintenance	tRNA wybutosine-synthesizing protein 3 structural maintenance of chromosome 3 DNA mismatch repair protein MLH3 chromosome transmission fidelity protein 18 high mobility group protein B1 callose synthase structural maintenance of chromosome 1 structural maintenance of chromosome 2	kinesin family member 18/19 tRNA (cytosine38-C5)-methyltransferase structural maintenance of chromosome 4 structural maintenance of chromosome 2 DNA excision repair protein ERCC-6 nijmegen breakage syndrome protein 1 nucleosome assembly protein 1-like 1 spastin structural maintenance of chromosome 3 structural maintenance of chromosome 1
Cell cycle regulation	ribonuclease P protein subunit POP4 microtubule-associated protein, RP/EB family CCR4-NOT transcription complex subunit 1 cell cycle checkpoint protein FUS-interacting serine-arginine-rich protein 1 pre-mRNA-splicing factor CWC22 cleavage and polyadenylation specificity factor subunit 2 CDK-activating kinase assembly factor MAT1 ER degradation enhancer, mannosidase alpha-like 1 centromere/kinetochore protein ZW10	protein neuralized small subunit ribosomal protein S13e FUS-interacting serine-arginine-rich protein 1 transitional endoplasmic reticulum ATPase cyclin B bromodomain-containing factor 1 E3 ubiquitin-protein ligase UHRF1 ubiquitin-conjugating enzyme E2 variant ribonuclease P protein subunit POP4 DNA polymerase alpha subunit B

Table A6. Cont.

Functional Category/Subcategory	Down-Regulated	UpRegulated
Cell growth	POZ domain-containing protein At2g30600 poly(A)-specific ribonuclease 26S proteasome non-ATPase regulatory subunit 10 preprotein translocase subunit YidC activation cell fate specification homeobox-leucine zipper protein root phototropism protein 3 sister chromatid cohesion protein PDS5	poly(A)-specific ribonuclease adenylate isopentenyltransferase 26S proteasome non-ATPase regulatory subunit 10 ATP-dependent RNA helicase DDX46/PRP5 respiratory burst oxidase L-ascorbate oxidase peptidyl-prolyl isomerase G (cyclophilin G) stress-induced-phosphoprotein 1 respiratory burst oxidase alpha-L-fucosidase
	Development	Tissue development protein phosphatase 2 solute carrier family 31 interleukin-1 receptor-associated kinase 4 neutral invertase multiple C2 and transmembrane domain-containing protein 2-like E3 ubiquitin-protein ligase BRE1 histidyl-tRNA synthetase nucleolin EID1-like F-box protein 3-like pleiotropic drug resistance protein 3-like
processes		cysteine synthase A protein-tyrosine phosphatase NAC domain-containing protein tropine dehydrogenase TCP4 beta-amyrin 24-hydroxylase antiviral helicase SKI2 U3 small nucleolar RNA-associated protein 4 phytochrome-interacting factor 3
Stress response	Response to metal tropine dehydrogenase ATP-binding cassette, subfamily B glutathione S-transferase serine/threonine-protein kinase PBS1 ATP-binding cassette, subfamily B crt homolog 1 circadian clock associated 1 pyridoxine 4-dehydrogenase	Ras-related protein Rab-1A jasmonate O-methyltransferase tyrosine 3-monooxygenase aspartate aminotransferase alcohol dehydrogenase (NADP+) glutathione S-transferase D-threo-aldose 1-dehydrogenase chaperonin GroEL CTP synthase copper-transporting atpase p-type
	Response to misfolded proteins	ubiquinol-cytochrome c reductase cytochrome c1 subunit calmodulin cell division cycle 20-like protein 1, cofactor of APC complex DUF246 domain-containing protein At1g04910 ubiquitin-conjugating enzyme E2 D/E

Table A6. Cont.

Functional Category/Subcategory	Down-Regulated	UpRegulated
Response to salts	aldose-6-phosphate reductase	beta-mannan synthase
	bromodomain-containing factor 1	V-type H ⁺ -transporting ATPase 21kDa
	bromodomain-containing protein 7/9	proteolipid subunit
	beta-mannan synthase	pectinesterase
	sterile alpha motif and leucine zipper containing kinase AZK	carboxymethylenebutenolidase
	outer membrane lipoprotein Blc	hydroquinone glucosyltransferase
	AIG2-like	peroxidase
	kynurenine formamidase-like	solute carrier family 15
	cyclin T	AP2-like factor, euAP2 lineage
	9-cis-epoxycarotenoid dioxygenase	speckle-type POZ protein
	extracellular signal-regulated kinase 1/2	

Top 10 DEGs in every sub-pathway were listed according to the differences range from large to small. The enzymes in some pathways less than 10, because of an enzyme could regulate by multi-genes.

Table A7. Main DEGs in amino acid biosynthesis pathways (gall vs. LWG).

	Down-Regulated	Up-Regulated
Histidine	imidazoleglycerol-phosphate dehydratase	histidinol-phosphatase histidinol-phosphate aminotransferase imidazole glycerol-phosphate synthase subunit HisF
Tryptophan	anthranilate synthase / indole-3-glycerol phosphate synthase anthranilate synthase	tryptophan synthase alpha chain anthranilate phosphoribosyltransferase
Tyrosine	cyclohexadieny/prephenate dehydrogenase Tyrosine aminotransferase	phenylalanine-4-hydroxylase aromatic-amino-acid transaminase chorismate mutase
Phenylalanine		prephenate dehydratase shikimate kinase 3-deoxy-7-phosphoheptulonate synthase
Serine		phosphoserine phosphatase phosphoserine aminotransferase
Cysteine	cysteine synthase serine O-acetyltransferase	
Methionine		5-methyltetrahydrofolate-homocysteine methyltransferase cysteine-S-conjugate beta-lyase cystathionine beta-synthase
Alanine	alanine transaminase	
Glutamine	glutamine synthetase	
Arginine	argininosuccinate synthase	
Proline	glutamate 5-kinase	pyrroline-5-carboxylate reductase glutamate-5-semialdehyde dehydrogenase
Valine	acetolactate synthase I/II/III large subunit	L-serine dehydratase dihydroxy-acid dehydratase branched-chain amino acid aminotransferase
Leucine		2-isopropylmalate synthase 3-isopropylmalate dehydrogenase branched-chain amino acid aminotransferase
Lysine		L-2-aminoadipate reductase kynurenine/2-aminoadipate aminotransferase diaminopimelate decarboxylase LL-diaminopimelate aminotransferase 4-hydroxy-tetrahydrodipicolinate reductase 4-hydroxy-tetrahydrodipicolinate synthase aspartate-semialdehyde dehydrogenase aspartate kinase

Table A8. Main DEGs in amino acid degradation pathways (gall vs. LWG).

	Down-Regulated	Up-Regulated
Tyrosine	tyrosine decarboxylase	
Phenylalanine	Phenylalanine dehydrogenase	
Serine		tryptophan synthase alpha chain
Cysteine	cysteine-S-conjugate beta-lyase cystathionine gamma-lyase S-adenosylmethionine decarboxylase	aspartate aminotransferase
Arginine		arginine decarboxylase
Proline	proline dehydrogenase	prolyl 4-hydroxylase
Threonine		L-serine/L-threonine ammonia-lyase
Glycine		glycine dehydrogenase

Table A9. Enzymes with the biggest difference in shikimate pathways (gall vs. LWG).

	Up-Regulated	Down-Regulated
Phenylpropanoid pathway	peroxidase 4-coumarate-CoA ligase 5-O-(4-coumaroyl)-D-quinic acid 3'-monooxygenase caffeic acid 3-O-methyltransferase trans-cinnamate 4-monooxygenase coniferyl-alcohol glucosyltransferase	cinnamyl-alcohol dehydrogenase ferulate-5-hydroxylase cinnamoyl-CoA reductase feruloyl-CoA 6-hydroxylase
Flavonols	flavonoid 3',5'-hydroxylase flavonoid 3'-monooxygenase isoflavone 7-O-glucoside-6''-O-malonyltransferase flavonol 3-O-methyltransferase	flavonol 3-O-glucosyltransferase
Isoflavonols	2-hydroxyisoflavanone dehydratase isoflavone-7-O-methyltransferase 2,7,4'-trihydroxyisoflavanone 4'-O-methyltransferase isoflavone 7-O-glucoside-6''-O-malonyltransferase isoflavone 7-O-glucosyltransferase	2-hydroxyisoflavanone synthase isoflavone/4'-methoxyisoflavone 2'-hydroxylase vestitone reductase
Anthocyanins	anthocyanidin 3-O-glucoside 2'''-O-xylosyltransferase anthocyanidin 5,3-O-glucosyltransferase	anthocyanidin 3-O-glucosyltransferase

Enzymes were listed according to the differences range from large to small.

Table A10. Enzymes with the biggest difference in plant-pathogen interaction pathways (LNG vs. LWG).

Up-Regulated	Down-Regulated
LRR receptor-like serine/threonine-protein kinase FLS2 disease resistance protein At4g27190-like WRKY transcription factor 2 cyclic nucleotide-gated ion channel 1 heat shock protein 83 disease resistance protein At4g27220 disease resistance protein RPS2	Di-glucose binding protein with Kinesin motor domain EIX receptor 1/2 calcium-dependent protein kinase 11 disease resistance protein TAO1-like

Enzymes were listed according to the differences range from large to small.

Table A11. The content of free amino acids and essential amino acids in different samples (Chao, 2020).

Samples	Free Amino Acids	Essential Amino Acids
Gall	3.098 + 0.001c	1.098 + 0.000c
LWG	2.928 + 0.001d	0.038 + 0.000d
LNG	3.230 + 0.001b	1.145 + 0.001b
aphids	4.796 + 0.002a	1.701 + 0.001a

References

- Rohfritsch, O.; Shorthouse, J.D. Insect Galls. In *Molecular Biology of Plant Tumors*; Academic Press: Cambridge, MA, USA, 1982.
- Stone, G.N.; Karsten, S. The adaptive significance of insect gall morphology. *Trends Ecol. Evol.* **2003**, *18*, 512–522. [[CrossRef](#)]
- Tooker, J.F.; Helms, A.M. Phytohormone Dynamics Associated with Gall Insects, and their Potential Role in the Evolution of the Gall-Inducing Habit. *J. Chem. Ecol.* **2014**, *40*, 742–753. [[CrossRef](#)] [[PubMed](#)]
- Ferreira, B.G.; Álvarez, R.; Bragança, G.P.; Alvarenga, D.R.; Pérez-Hidalgo, N.; Isaias, R.M.S. Feeding and Other Gall Facets: Patterns and Determinants in Gall Structure. *Bot. Rev.* **2019**, *85*, 78–106. [[CrossRef](#)]
- Álvarez, R.; Encina, A.; Hidalgo, N.P. Histological aspects of three *Pistacia terebinthus* galls induced by three different aphids: *Paracletus cimiciformis*, *Forda marginata* and *Forda formicaria*. *Plant Sci.* **2009**, *176*, 303–314. [[CrossRef](#)]
- Stone, G.N.; Schönrogge, K.; Atkinson, R.J.; Bellido, D.; Pujade-Villar, J. The Population Biology of Oak Gall Wasps (Hymenoptera: Cynipidae). *Annu. Rev. Entomol.* **2002**, *47*, 633–668. [[CrossRef](#)]
- Wool, D. GALLIN GAPHIDS: Specialization, Biological Complexity, and Variation. *Annu. Rev. Entomol.* **2004**, *49*, 175–192. [[CrossRef](#)] [[PubMed](#)]
- Morris, D.C.; Schwarz, M.P.; Cooper, S.J.B.; Mound, L.A. Phylogenetics of Australian Acacia thrips: The evolution of behaviour and ecology. *Mol. Phylogenet. Evol.* **2002**, *25*, 278–292. [[CrossRef](#)]
- Blanche, K.R. Diversity of insect-induced galls along a temperature- rainfall gradient in the tropical savannah region of the Northern Territory, Australia. *Austral Ecol.* **2000**, *25*, 42. [[CrossRef](#)]
- Donald, G.M.I.; Ivey, C.T.; Shedd, J.D. Support for the microenvironment hypothesis for adaptive value of gall induction in the California gall wasp, *Andricus quercuscalifornicus*. *Entomol. Exp. Appl.* **2009**, *132*, 126–133. [[CrossRef](#)]
- Alvarez, R.; Molist, P.; González-Sierra, S.; Martínez, J.J.I.; Nafria, J.M.N. The histo structure of galls induced by aphids as a useful taxonomic character: The case of *Rectinasus* (Hemiptera, Aphididae, Eriosomatinae). *Zootaxa* **2014**, *3861*, 487–492. [[CrossRef](#)]
- Costello, J.F. Methylation matters. *J. Med. Genet.* **2001**, *38*, 285–303. [[CrossRef](#)] [[PubMed](#)]
- Martinez, J.J.I. Anti-insect effects of the gall wall of *Baizongia pistaciae* [L.], a gall-inducing aphid on *Pistacia palaestina* Boiss. *Arthropod Plant Interact.* **2010**, *4*, 29–34. [[CrossRef](#)]
- Shorthouse, J.D.; Wool, D.; Raman, A. Gall-inducing insects—Nature’s most sophisticated herbivores. *Basic Appl. Ecol.* **2005**, *6*, 407–411. [[CrossRef](#)]
- Nabity, P.D.; Haus, M.J.; Berenbaum, M.R.; DeLucia, E.H. Leaf-galling phylloxera on grapes reprograms host metabolism and morphology. *Proc. Natl. Acad. Sci. USA* **2013**, *110*, 16663–16668. [[CrossRef](#)]
- Fay, P.A.; Hartnett, D.C.; Knapp, A.K. Increased photosynthesis and water potentials in *Silphium integrifolium* galled by cynipid wasps. *Oecologia* **1993**, *93*, 114–120. [[CrossRef](#)] [[PubMed](#)]
- Moseley, C.T.; Cramer, M.D.; Hoffmann, C.A.K.H. Why does Dasineura dielsi-induced galling of Acacia cyclops not impede vegetative growth? *J. Appl. Ecol.* **2009**, *46*, 214–222. [[CrossRef](#)]
- Andersen, P.C.; Mizell, R.F. Physiological Effects of Galls Induced by *Phylloxera notabilis* (Homoptera: Phylloxeridae) on Pecan Foliage. *Environ. Entomol.* **1987**, *16*, 264–268. [[CrossRef](#)]
- Florentine, S.K.; Raman, A.; Dhileepan, K. Effects of Gall Induction by Epiblema Strenuana on Gas Exchange, Nutrients, and Energetics in Parthenium Hysterophorus. *BioControl* **2005**, *50*, 787–801. [[CrossRef](#)]
- Wingler, A.; Roitsch, T. Metabolic regulation of leaf senescence: Interactions of sugar signalling with biotic and abiotic stress responses. *Plant Biol.* **2008**, *10*, 50–62. [[CrossRef](#)] [[PubMed](#)]
- Morkunas, I.; Mai, V.C.; Gabryś, B. Phytohormonal signaling in plant responses to aphid feeding. *Acta Physiol. Plant.* **2011**, *33*, 2057–2073. [[CrossRef](#)]
- Chen, H.; Liu, J.; Cui, K.; Lu, Q.; Wang, C.; Wu, H.; Yang, Z.; Ding, W.; Shao, S.; Wang, H.; et al. Molecular mechanisms of tannin accumulation in Rhus galls and genes involved in plant-insect interactions. *Sci. Rep.* **2018**, *8*, 9841. [[CrossRef](#)] [[PubMed](#)]
- Yang, Z. *High Yield Cultivation Technology of Chinese Gallnut*; China Forestry Press: Beijing, China, 2011.
- Shao, S.-X.; Yang, Z.-X.; Chen, X.-M. Gall development and clone dynamics of the galling aphid *Schlechtendalia chinensis* (Hemiptera: Pemphigidae). *J. Econ. Entomol.* **2013**, *106*, 1628–1637. [[CrossRef](#)]
- Chen, X.; Yang, Z.; Chen, H.; Qi, Q.; Liu, J.; Wang, C.; Shao, S.; Lu, Q.; Li, Y.; Wu, H.; et al. A Complex Nutrient Exchange Between a Gall-Forming Aphid and Its Plant Host. *Front. Plant Sci.* **2020**, *11*, 811. [[CrossRef](#)]

26. Gonzalez, P.S.; O'Prey, J.; Cardaci, S.; Barthelet, V.J.A.; Sakamaki, J.-I.; Beaumatin, F.; Roseweir, A.; Gay, D.M.; Mackay, G.; Malviya, G.; et al. Mannose impairs tumour growth and enhances chemotherapy. *Nature* **2018**, *563*, 719–723. [[CrossRef](#)]
27. Cai, W.; Pang, X.; Hua, B.; Liang, G.; Song, D. *Basic Entomology*; China Agricultural University Press: Beijing, China, 2001.
28. French, D. Chemical and Physical Properties of Starch. *J. Anim. Sci.* **1973**, *37*, 1048–1061. [[CrossRef](#)] [[PubMed](#)]
29. Nowak, H.; Komor, E. How aphids decide what is good for them: Experiments to test aphid feeding behaviour on *Tanacetum vulgare* (L.) using different nitrogen regimes. *Oecologia* **2010**, *163*, 973–984. [[CrossRef](#)] [[PubMed](#)]
30. Wang, C.; Chen, X.-M.; Yang, Z.-X.; Chen, H.; Shao, S.-X.; Wu, H.-X. Studies on free amino acids of aphid *Schlechtendalia chinensis* and the host plant *Rhus chinensis*. *For. Res.* **2018**, *31*, 114–119. [[CrossRef](#)]
31. Wu, H.-X.; Chen, X.; Chen, H.; Lu, Q.; Yang, Z.; Ren, W.; Liu, J.; Shao, S.; Wang, C.; King-Jones, K.; et al. Variation and diversification of the microbiome of *Schlechtendalia chinensis* on two alternate host plants. *PLoS ONE* **2018**, *13*, e0200049. [[CrossRef](#)]
32. Mashiguchi, K.; Hisano, H.; Takeda-Kamiya, N.; Takebayashi, Y.; Ariizumi, T.; Gao, Y.; Ezura, H.; Sato, K.; Zhao, Y.; Hayashi, K.-I.; et al. *Agrobacterium tumefaciens* Enhances Biosynthesis of Two Distinct Auxins in the Formation of Crown Galls. *Plant Cell Physiol.* **2019**, *60*, 29–37. [[CrossRef](#)]
33. Zhang, H.; Lang, Z.; Zhu, J.-K. Dynamics and function of DNA methylation in plants. *Nat. Rev. Mol. Cell Biol.* **2018**, *19*, 489–506. [[CrossRef](#)]
34. Rawat, N.; Neeraja, C.N.; Nair, S.; Bentur, J.S. Differential gene expression in gall midge susceptible rice genotypes revealed by suppressive subtraction hybridization (SSH) cDNA libraries and microarray analysis. *Rice* **2012**, *5*, 1–15. [[CrossRef](#)]
35. Zhu, L.; Liu, X.; Liu, X.; Jeannotte, R.; Reese, J.C.; Harris, M.; Stuart, J.J.; Chen, M.-S. Hessian Fly (*Mayetiola destructor*) Attack Causes a Dramatic Shift in Carbon and Nitrogen Metabolism in Wheat. *Mol. Plant Microbe Interact.* **2007**, *21*, 70–78. [[CrossRef](#)]
36. Gonzáles, W.L.; Fernández, R. Do host plant traits and galling insects affect the abundance of *Issus* sp. on *Colliguaja odorifera* Mol. along an altitudinal gradient? *Rev. Chil. Entomol.* **2000**, *26*, 93–95.
37. Guo, R.; Wang, Y.P.; Hong, W.U. The diversity of insects galls and relationships between insects galls and their host plants and environment. *J. Environ. Entomol.* **2012**, *34*, 370–376.
38. Lu, Q.; Chen, H.; Wang, C.; Yang, Z.-X.; Lü, P.; Chen, M.-S.; Chen, X.-M. Macro- and Microscopic Analyses of Anatomical Structures of Chinese Gallnuts and Their Functional Adaptation. *Sci. Rep.* **2019**, *9*, 5193. [[CrossRef](#)] [[PubMed](#)]
39. Larson, K.C.; Whitham, T.G. Manipulation of food resources by a gall-forming aphid: The physiology of sink-source interactions. *Oecologia* **1991**, *88*, 15–21. [[CrossRef](#)]
40. Grabherr, M.G.; Haas, B.J.; Yassour, M.; Levin, J.Z.; Thompson, D.A.; Amit, I.; Adiconis, X.; Fan, L.; Raychowdhury, R.; Zeng, Q.; et al. Full-length transcriptome assembly from RNA-Seq data without a reference genome. *Nat. Biotechnol.* **2011**, *29*, 644–652. [[CrossRef](#)] [[PubMed](#)]